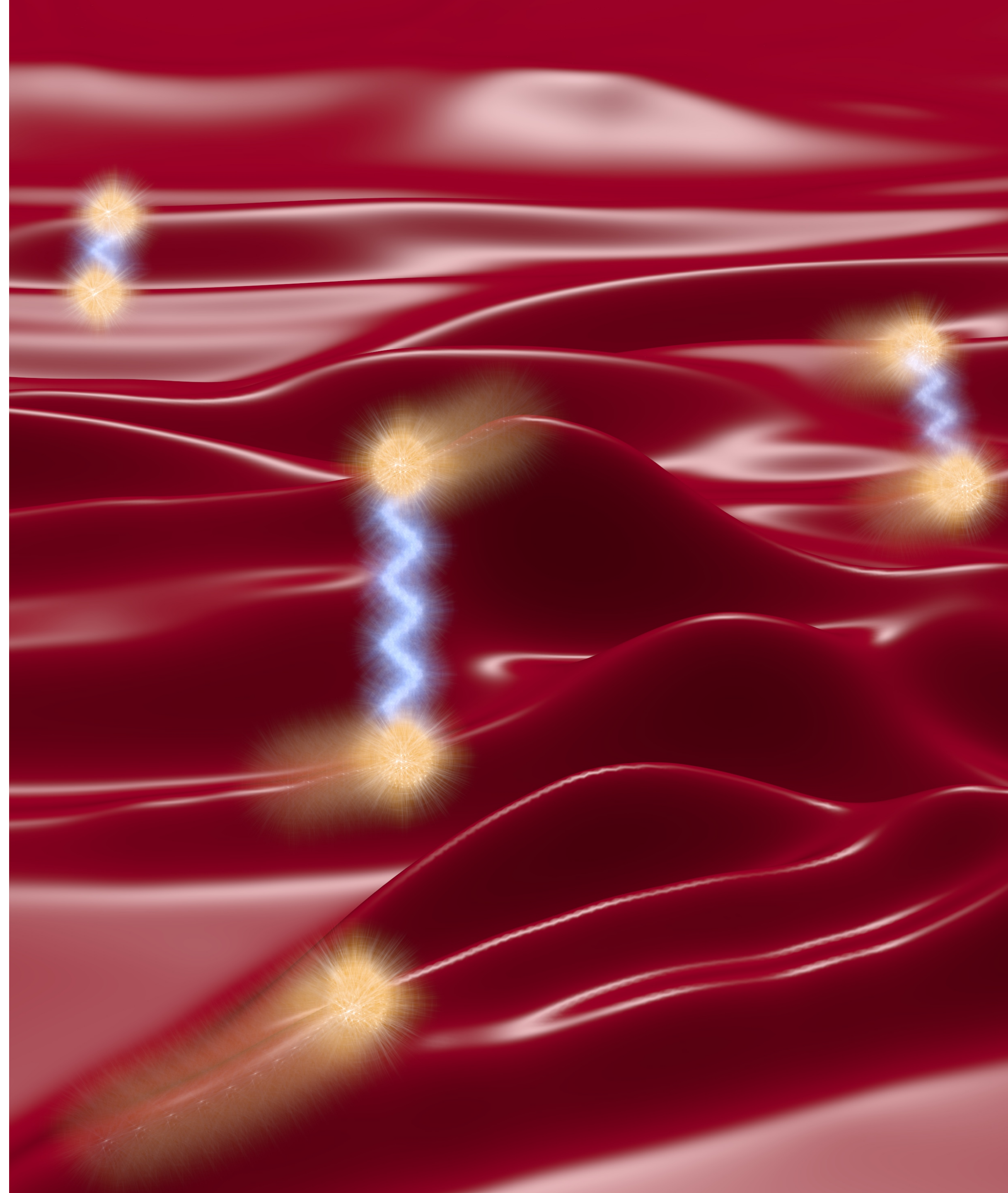




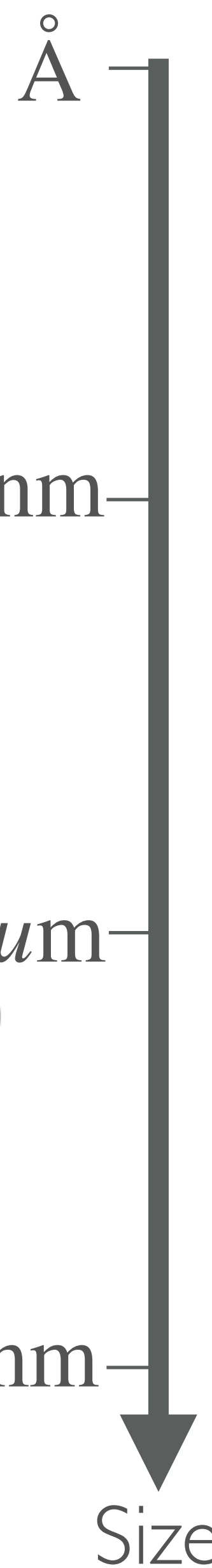
QUANTUM ESPRESSO:

from density-functional theory to
dual wave-particle transport and
device simulation

Michele Simoncelli
ms2855@cam.ac.uk



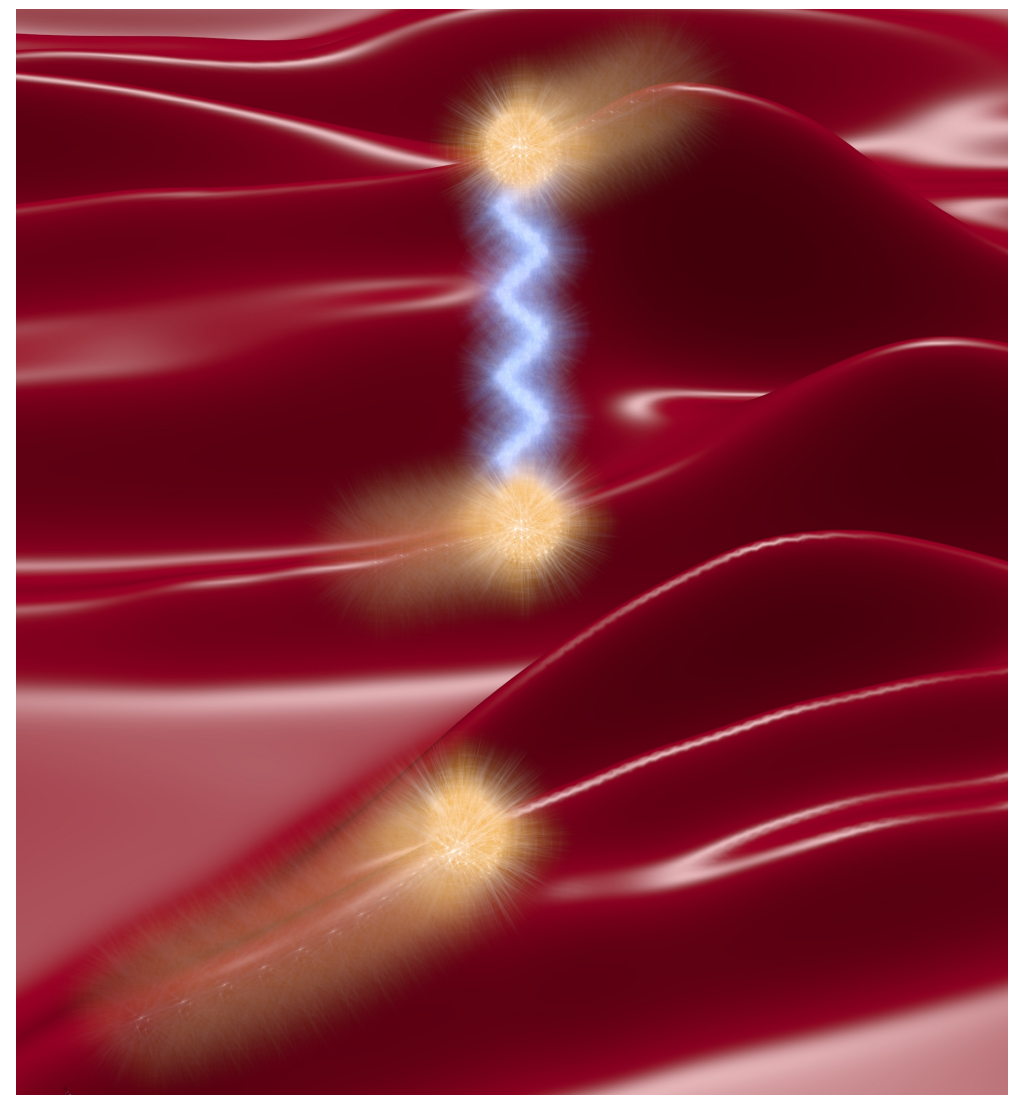
OUTLINE



Density functional theory and dual wave-particle transport

Wigner formulation for electron and phonon transport

Simoncelli, Marzari, Mauri, Nat. Phys. 15 (2019)
Simoncelli, Marzari, Mauri, Phys. Rev. X 12 (2022)
Cepellotti and Kozinsky, Materials Today Physics 19 (2021)



Raman spectra: structural & quasiparticles' properties

Beyond band transport

Charge transport in solid state ionic conductors

Kahle, Marcolongo, & Marzari, Energy Environ. Sci. 13 (2020)

Thermal transport in glasses from first principles

Simoncelli, Mauri, Marzari, npj Comput. Mater. 9 (2023);
Harper, Iwanowski, Payne, Simoncelli arXiv 2303.08637 (2023)



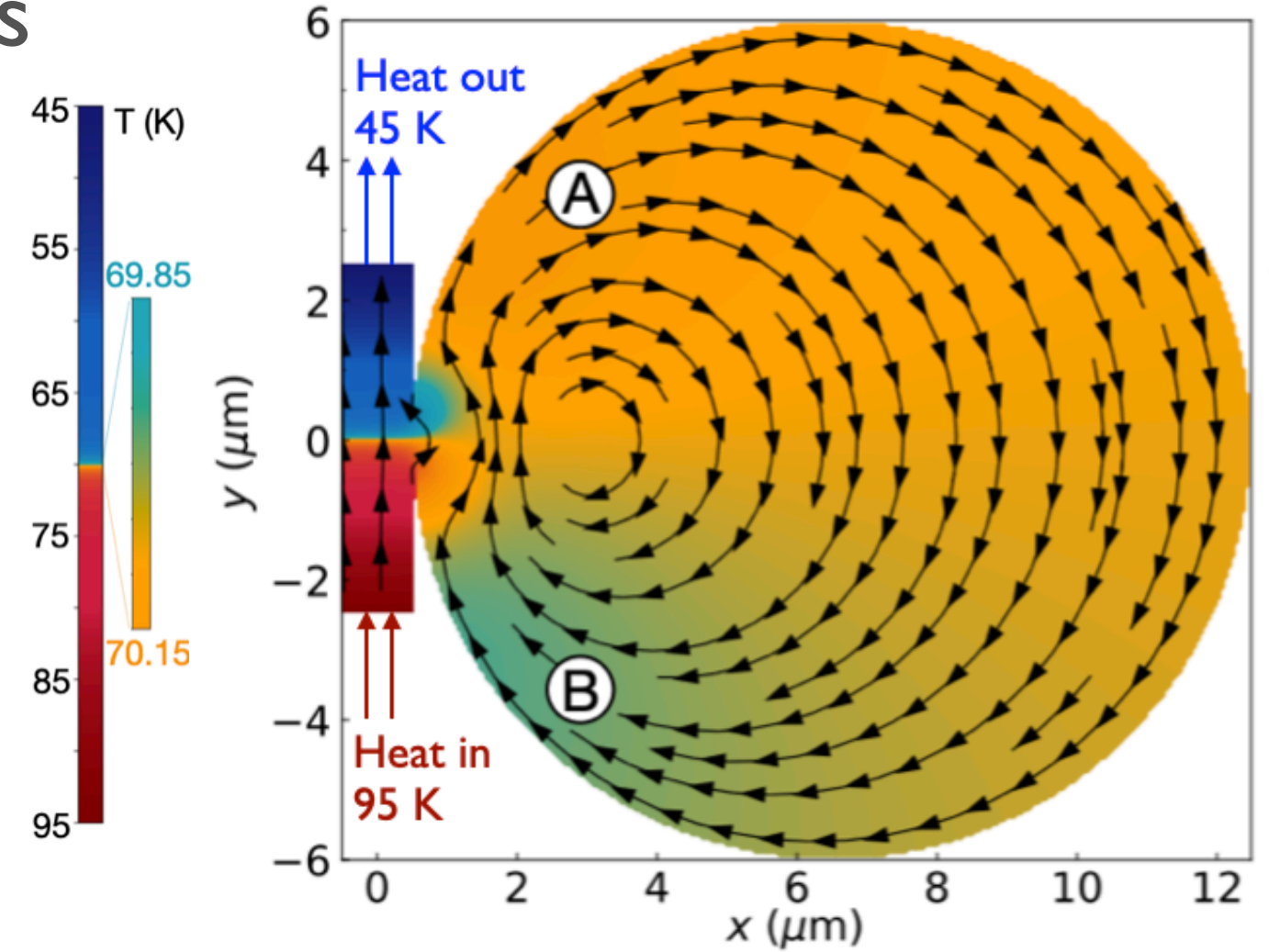
First-principles parametrisation of mesoscopic models

Viscous heat equations & diffusive-hydrodynamic crossover

Simoncelli, Marzari, Cepellotti, Phys. Rev. X 10 (2020)
Dragašević and Simoncelli, arXiv:2303.12777 (23.03.2023)

Predicting reflectivity and colour of metals

Prandini, Rignanese, & Marzari, npj Comput. Mater. 129 (2019)





Quantum opEn-Source Package for Research in Electronic Structure, Simulation, and Optimization

J. Phys.: Condens. Matter 21, 395502 (2009) and J. Phys.: Condens. Matter 29, 465901 (2017)

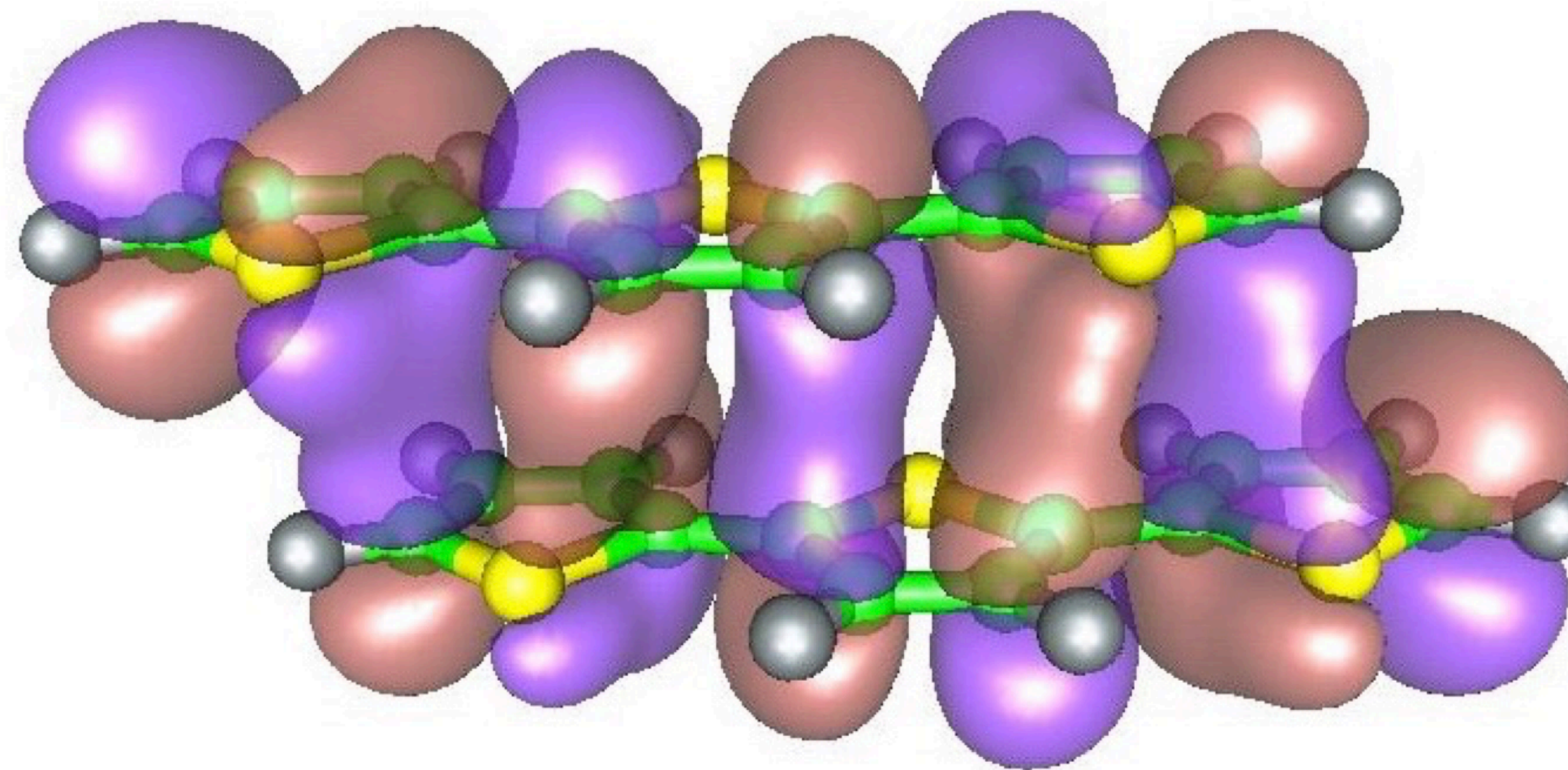
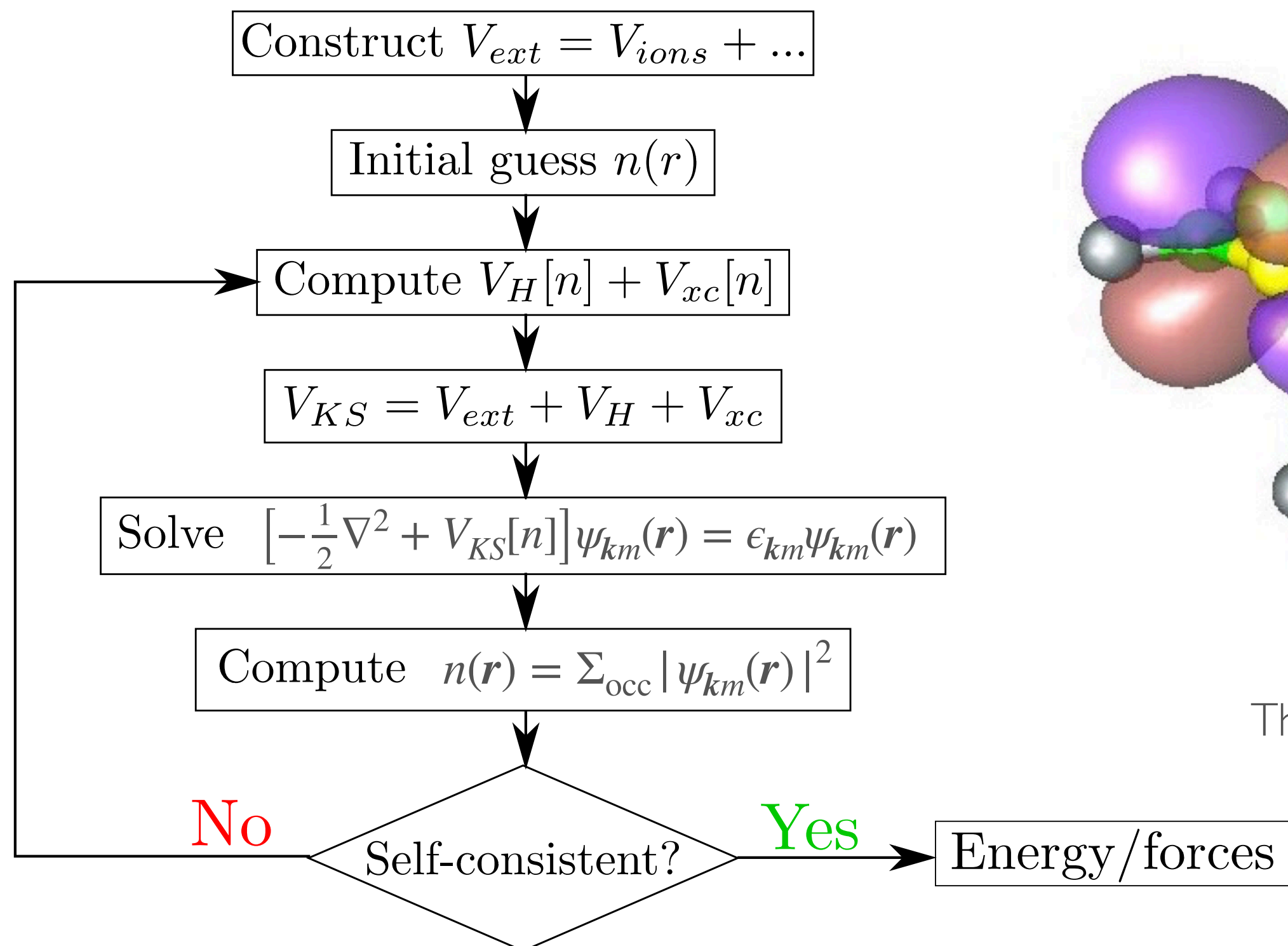
Composed of several packages:

- CP:** Car-Parrinello molecular dynamics
- PWneb:** Nudged Elastic Band (NEB) for reaction pathways and barriers
- atomic:** pseudopotential generation code
- PWcond:** ballistic conductance
- XSpectra:** Calculation of X-ray near-edge adsorption spectra (XANES)
- GWL:** GW band structure with ultralocalized Wannier functions
- TD-DFPT:** Time-Dependent Density-Functional Perturbation Theory
- HP:** Hubbard parameters from linear response
- turboMagnon:** spin-wave spectra using TD-DFPT
- PWscf:** self-consistent electronic structure, structural optimization, molecular dynamics
- PHonon:** linear-response calculations (phonons, dielectric properties)
- D3Q:** Phonon-phonon interaction and thermal conductivity
- EPW:** Electron-phonon coefficients and related properties

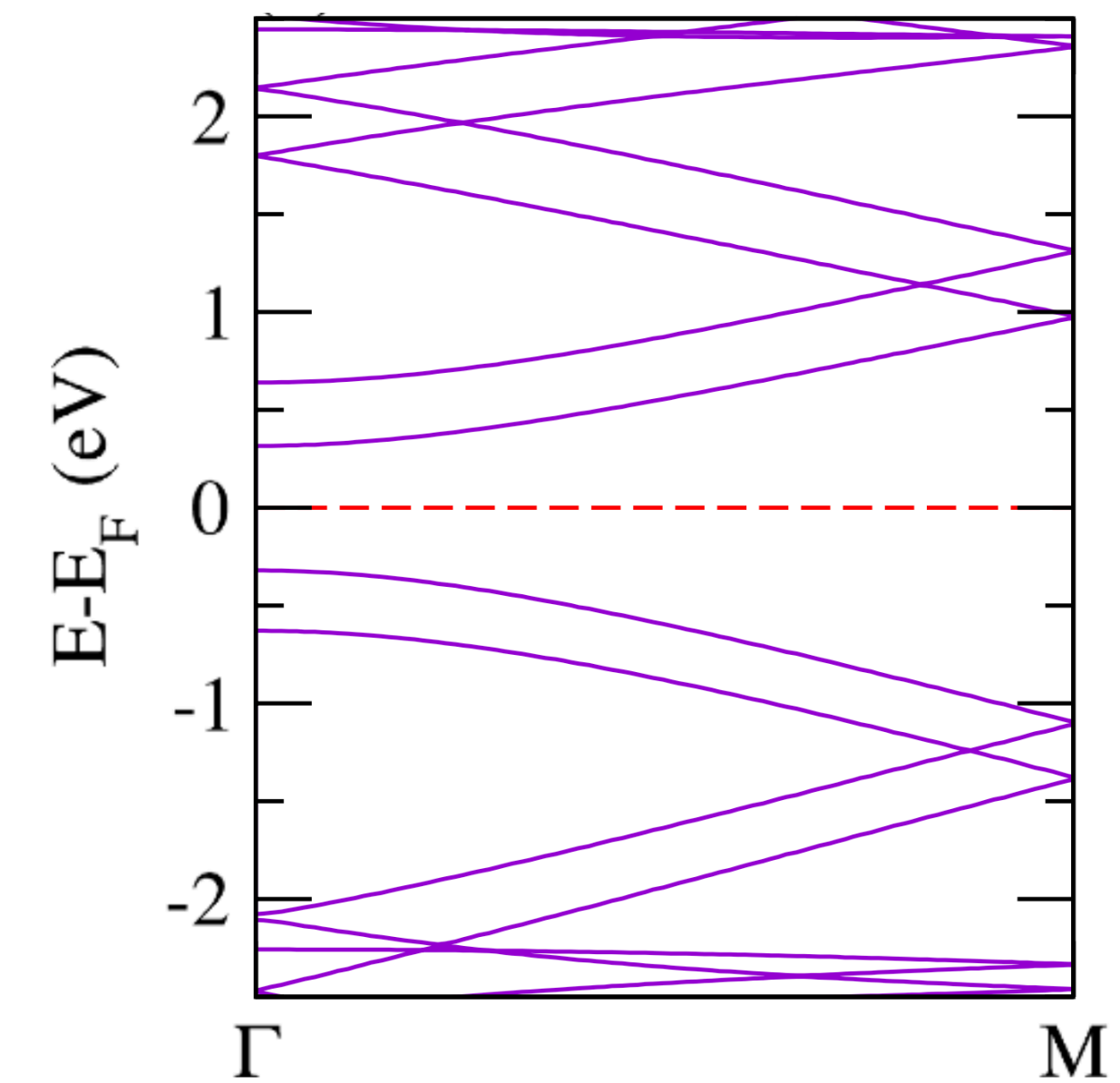
CHARGE DENSITY AND BAND STRUCTURE

Ground state electronic energy and density, $n(\mathbf{r}) = \sum_{km \in \text{Occ}} |\psi_{km}(\mathbf{r})|^2$

Self-consistent solution of Kohn Sham equation: $\left[-\frac{1}{2}\nabla^2 + V_{\text{ext}} + V_H[n] + V_{xc}[n] \right] \psi_{km}(\mathbf{r}) = \epsilon_{km} \psi_{km}(\mathbf{r})$



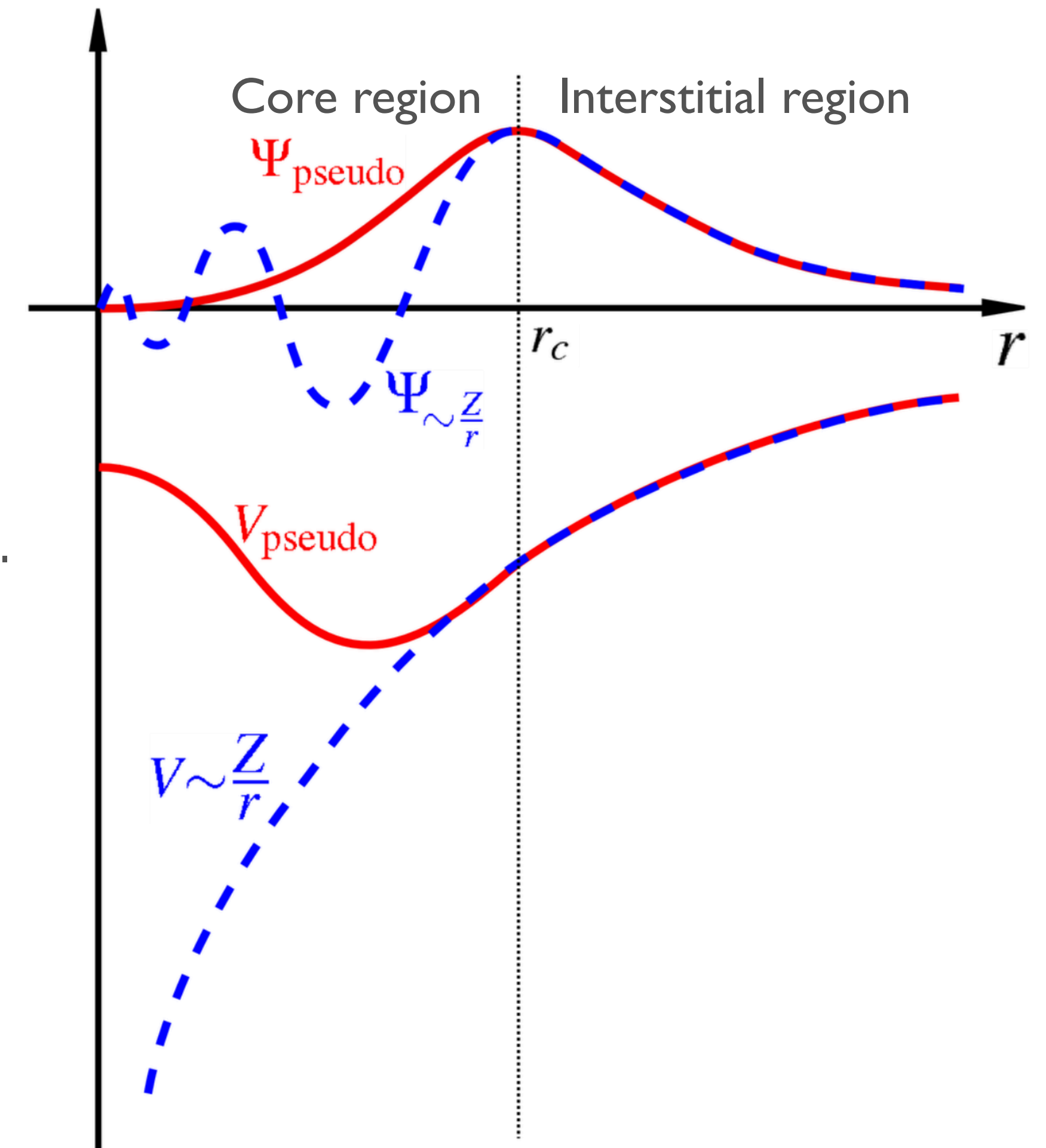
Thiophene (C₄H₄S), Scherlis and Marzari, JPCB (2004)



Kaloni et al, Sci. Rep. 6, 36554 (2016)

PSEUDOPOTENTIALS — SSSP LIBRARY

- Valence wavefunctions are ‘soft and smooth’ in the interstitial region, they strongly oscillate in the core region;
- Bonds are mainly determined by $\Psi_{km}(\mathbf{r})$ in the interstitial region;
- Core electrons are very localized;
- Approximation to reduce computational cost: freeze the core electrons & replace the real ionic potential with a ‘pseudopotential’.



SSSP Efficiency (version 1.3.0)

Note: The Ir (Iridium) pseudopotential of the efficiency library has a ghost state at ~10 eV above the Fermi energy, please use it with caution.

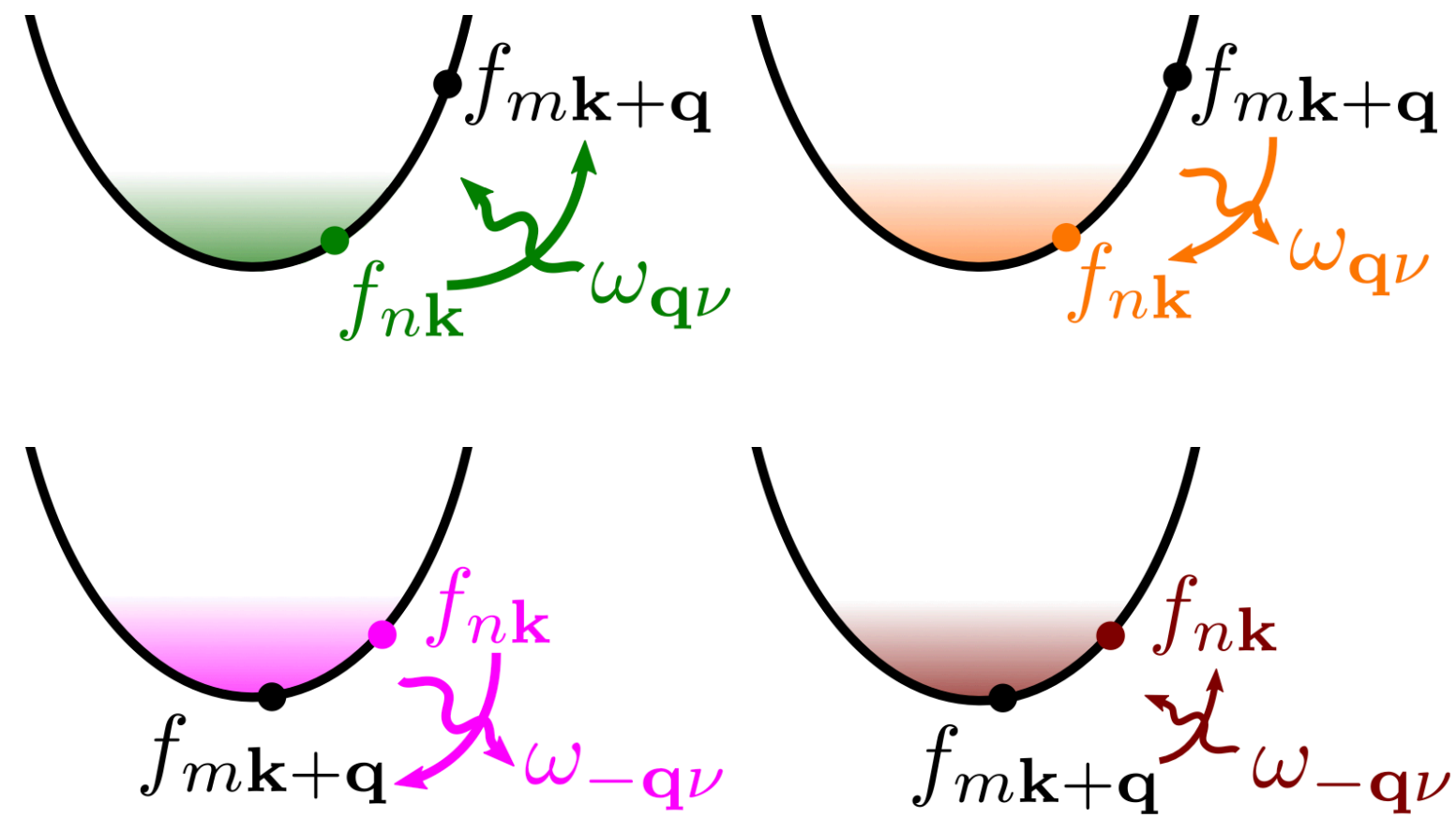
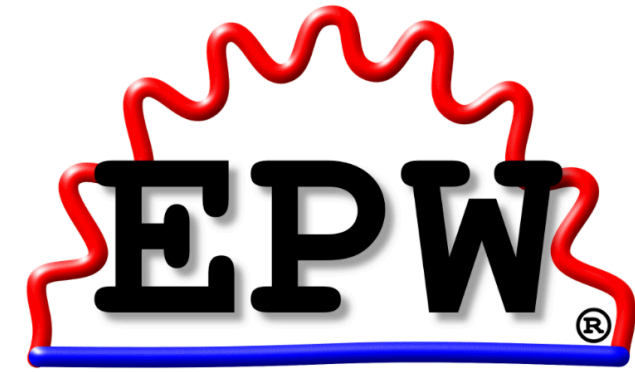
[↓ Cutoffs table](#) [↓ Pseudos](#) [Switch to SSSP Precision](#)

<https://www.materialscloud.org/discover/sssp>

H ₆₀₍₄₈₀₎																	He ₅₀				
Li ₄₀₍₃₂₀₎	Be ₄₀															B ₃₅₍₂₈₀₎	C ₄₅₍₃₆₀₎	N ₆₀₍₄₈₀₎	O ₅₀₍₄₀₀₎	F ₄₅₍₃₆₀₎	Ne ₅₀
Na ₄₀	Mg ₂₀															Al ₃₀₍₂₄₀₎	Si ₃₀₍₂₄₀₎	P ₃₀₍₂₄₀₎	S ₃₅₍₂₈₀₎	Cl ₄₀₍₃₂₀₎	Ar ₆₀₍₂₄₀₎
K ₆₀₍₄₈₀₎	Ca ₂₀	Sc ₄₀₍₁₆₀₎	Ti ₃₅₍₂₈₀₎	V ₃₅₍₂₈₀₎	Cr ₄₀₍₃₂₀₎	Mn ₆₅	Fe ₆₀	Co ₄₅	Ni ₄₅₍₃₆₀₎	Cu ₆₀	Zn ₄₀₍₃₂₀₎	Ga ₇₀	Ge ₄₀	As ₃₅₍₂₈₀₎	Se ₂₀	Br ₃₀₍₂₄₀₎	Kr ₄₅₍₁₈₀₎				
Rb ₂₀	Sr ₃₀₍₂₄₀₎	Y ₃₅₍₂₈₀₎	Zr ₃₀₍₂₄₀₎	Nb ₄₀	Mo ₂₅	Tc ₃₀₍₁₂₀₎	Ru ₂₅	Rh ₃₅	Pd ₄₅	Ag ₅₀	Cd ₆₀	In ₅₀₍₄₀₀₎	Sn ₆₀	Sb ₄₀	Te ₃₀₍₂₄₀₎	I ₃₅₍₂₈₀₎	Xe ₆₀				
Cs ₂₀	Ba ₂₀	*	Hf ₅₀₍₂₀₀₎	Ta ₄₅₍₃₆₀₎	W ₃₀₍₂₄₀₎	Re ₂₀	Os ₄₀	Ir ₅₅₍₄₄₀₎	Pt ₃₅₍₂₈₀₎	Au ₄₅	Hg ₅₀	Tl ₅₀₍₄₀₀₎	Pb ₄₀	Bi ₄₅₍₃₆₀₎	Po ₇₅	At ₈₀₍₆₄₀₎	Rn ₁₂₀				
Fr ₁₅₀	Ra ₈₀	**																			
		*	La ₄₀₍₃₂₀₎	Ce ₅₀	Pr ₄₀₍₃₂₀₎	Nd ₄₀	Pm ₄₀	Sm ₄₀	Eu ₄₀	Gd ₄₀	Tb ₄₀₍₃₂₀₎	Dy ₄₀	Ho ₄₀	Er ₄₀₍₃₂₀₎	Tm ₄₀	Yb ₄₀	Lu ₄₅₍₃₆₀₎				
		**	Ac ₄₀₍₃₂₀₎	Th ₆₀₍₄₈₀₎	Pa ₆₀	U ₆₀₍₄₈₀₎	Np ₆₀	Pu ₆₀	Am ₆₀	Cm ₆₀	Bk ₆₀₍₄₈₀₎	Cf ₆₀₍₄₈₀₎	Es ₆₀₍₄₈₀₎	Fm ₆₀	Md ₆₀	No ₆₀	Lr ₆₀₍₄₈₀₎				

INTERACTIONS: BROADENING OF BANDS

Electron-phonon interaction

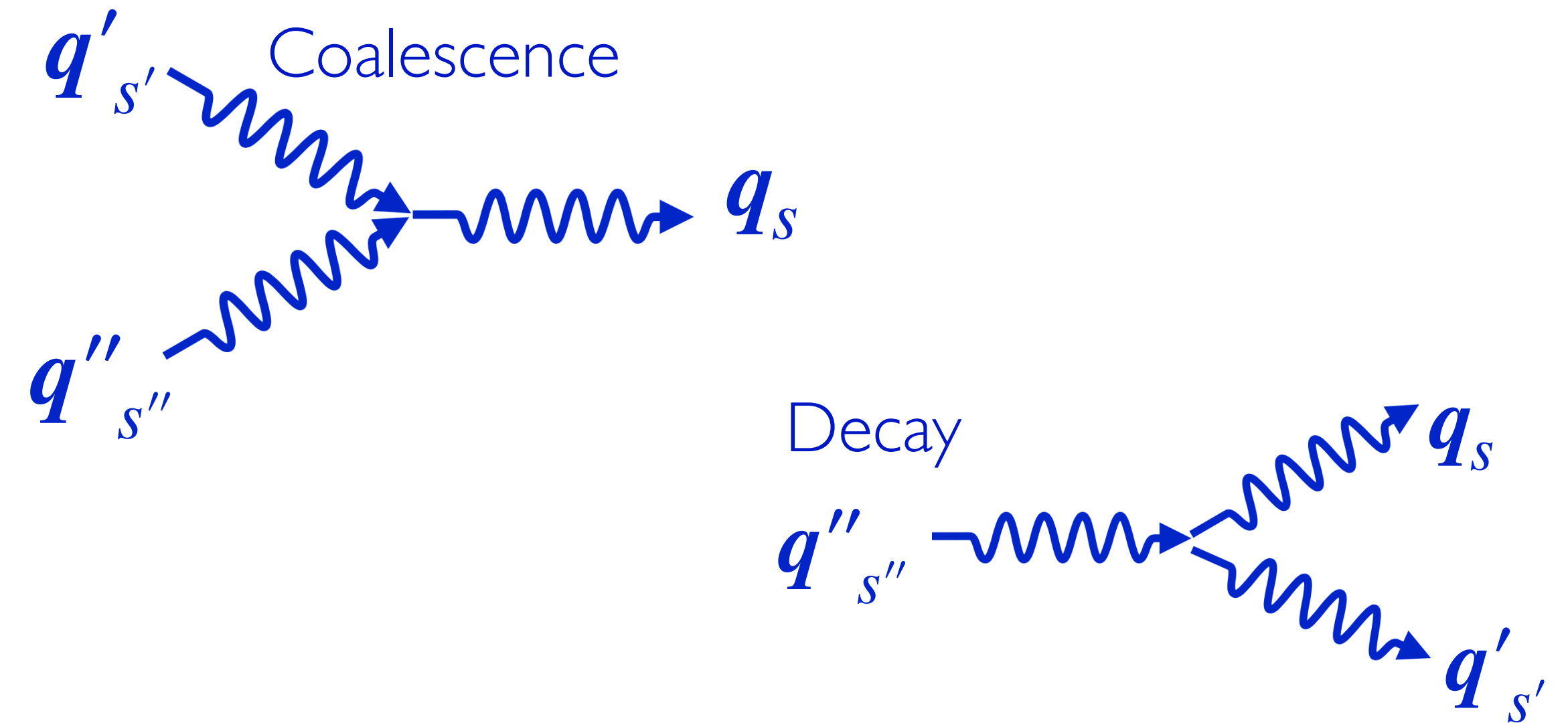


Electron-phonon matrix element $g_{m,m',s}(\mathbf{k}, \mathbf{k}', \mathbf{q}) = \sqrt{\frac{\hbar}{2M_0\omega_{qs}}} \langle \psi_{\mathbf{k}'m'} | \partial_{\mathbf{q}s} V | \psi_{\mathbf{k}m} \rangle$

Self-consistent potential associated with phonon $\mathbf{q}s$

Poncé et al. *Computer Phys. Commun.*, 209 (2016)
 Poncé et al. *Rep. Prog. Phys.* 83 036501 (2020)

Phonon-phonon interaction



phonon-phonon matrix element

$$|V^{(3)}(\mathbf{q}s, -\mathbf{q}'s', -\mathbf{q}''s'')|^2$$

Third derivative of the Born-Oppenheimer potential

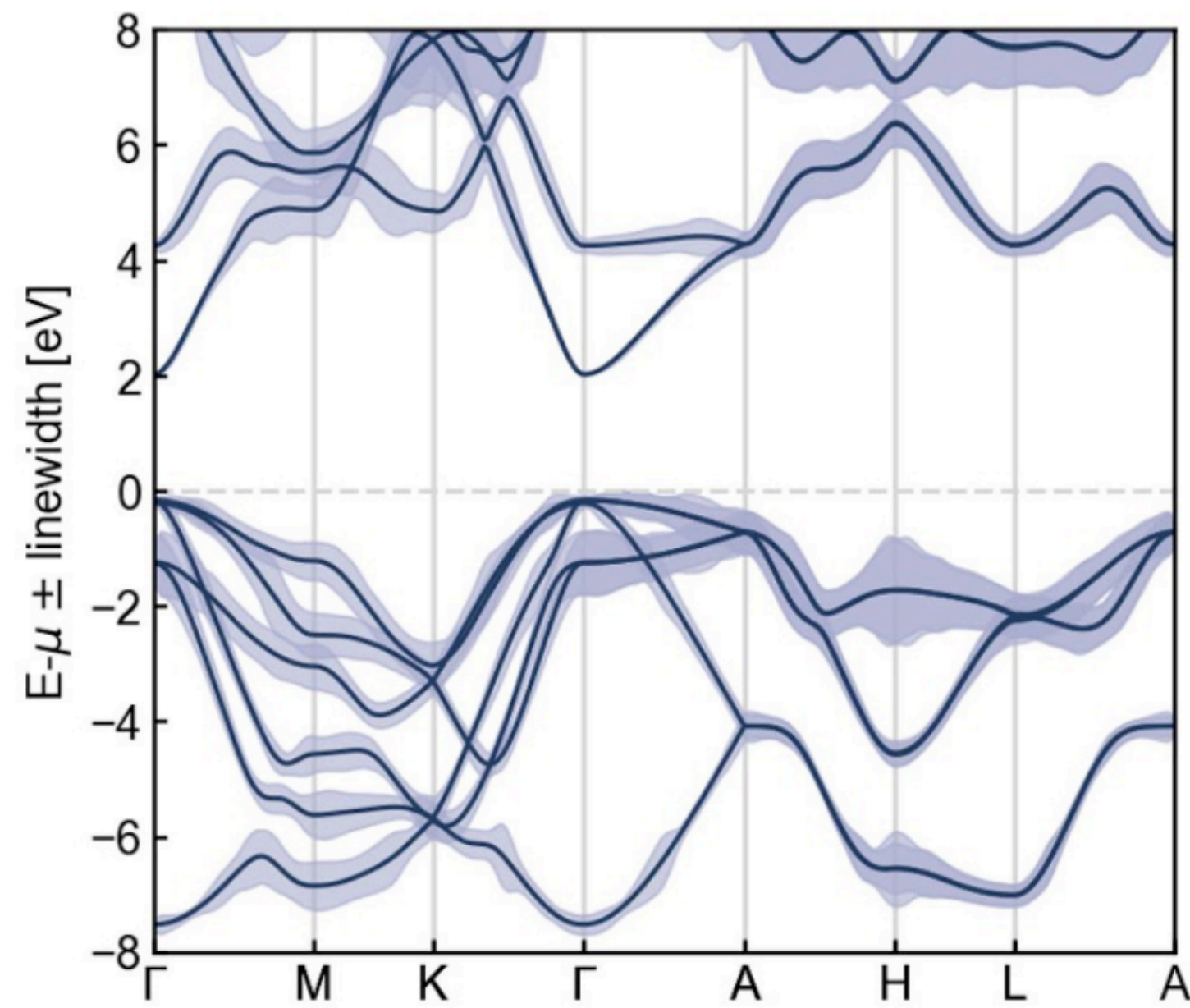
Paulatto et al. *PRB* 87 (2013)
 Fugallo et al. *PRB* 88 (2013)

'BROADENED' BAND STRUCTURE FROM DFT

Electrons

— $\epsilon(\mathbf{k})_m$

$$\Gamma(\mathbf{k})_m = \frac{1}{\mathcal{N}_k \mathcal{V}} \sum_{\mathbf{k}'' m'', \mathbf{q}s} \frac{2\pi}{\hbar} |g_{m, m'', s}(\mathbf{k}, \mathbf{k}'', \mathbf{q})|^2 \delta_{\mathbf{k}'' - \mathbf{k} - \mathbf{q}, \mathbf{G}} \left[(\bar{N}(\mathbf{q})_s + \bar{F}(\mathbf{k}'')_{m''}) \times \delta[\epsilon(\mathbf{k}'')_{m''} - \epsilon(\mathbf{k})_m - \hbar\omega(\mathbf{q})_s] + (1 - \bar{F}(\mathbf{k}'')_{m''} + \bar{N}(\mathbf{q})_s) \delta[\epsilon(\mathbf{k}'')_{m''} - \epsilon(\mathbf{k})_m + \hbar\omega(\mathbf{q})_s] \right]$$

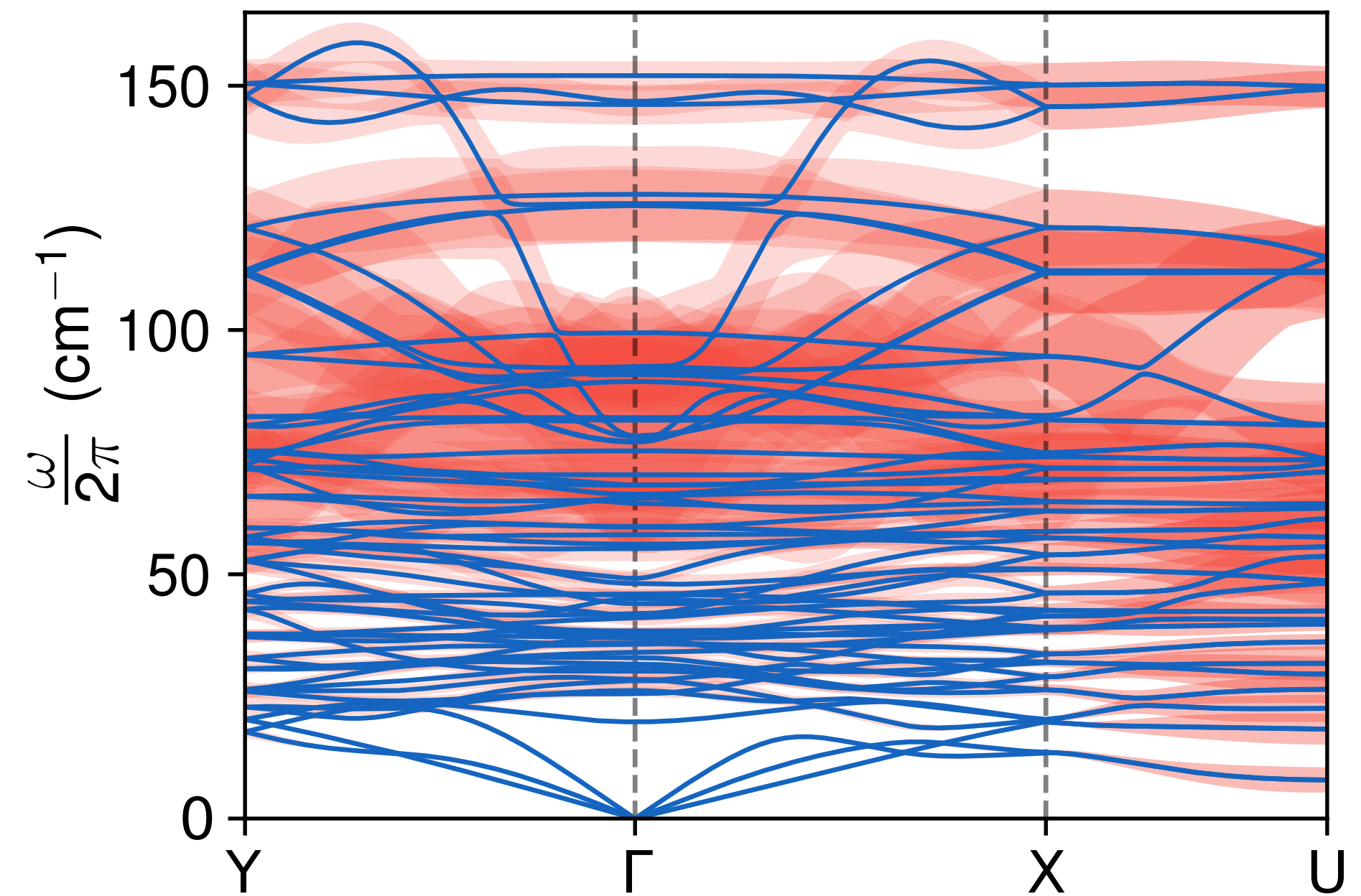


GaN, from Cepellotti et al, *J. Phys. Mater.* 5 (2022)

Phonons

— $\omega(\mathbf{q})_s$

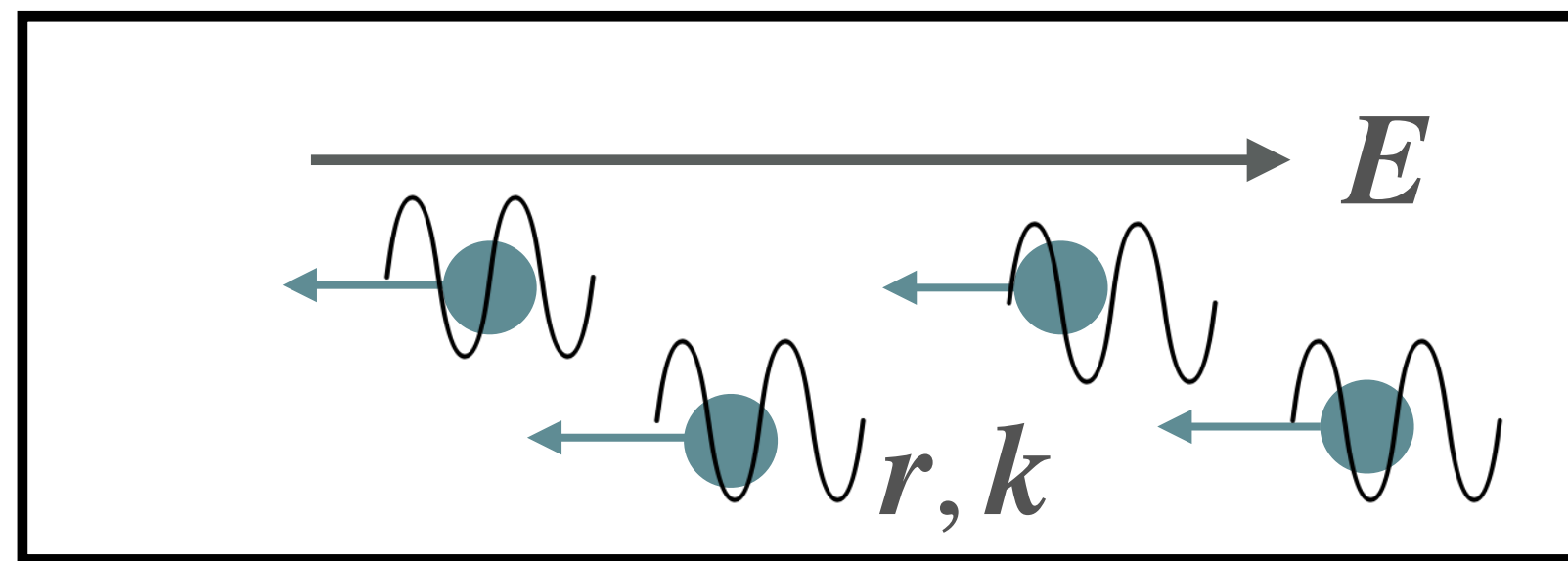
$$\Gamma(\mathbf{q})_s = \frac{36\pi}{\hbar N_q} \sum_{\mathbf{q}, \mathbf{q}', s, s'} |V^{(3)}(\mathbf{q}s, -\mathbf{q}'s', -\mathbf{q}''s'')|^2 \delta_{\mathbf{q} - \mathbf{q}' - \mathbf{q}'', \mathbf{G}} \left[(\bar{N}_{\mathbf{q}'s'} + \bar{N}_{\mathbf{q}''s''} + 1) \times \delta(\hbar\omega_{\mathbf{q}s} - \hbar\omega_{\mathbf{q}'s'} - \hbar\omega_{\mathbf{q}''s''}) + (\bar{N}_{\mathbf{q}'s'} - \bar{N}_{\mathbf{q}''s''}) [\delta(\hbar\omega_{\mathbf{q}s} + \hbar\omega_{\mathbf{q}'s'} - \hbar\omega_{\mathbf{q}''s''}) - \delta(\hbar\omega_{\mathbf{q}s} - \hbar\omega_{\mathbf{q}'s'} + \hbar\omega_{\mathbf{q}''s''})] \right]$$



CsPbBr₃, from **Simoncelli**, Marzari, Mauri, *Nat. Phys.* 15 (2019)

FROM BAND STRUCTURE TO TRANSPORT COEFFICIENTS

Wigner transport equation for electrons



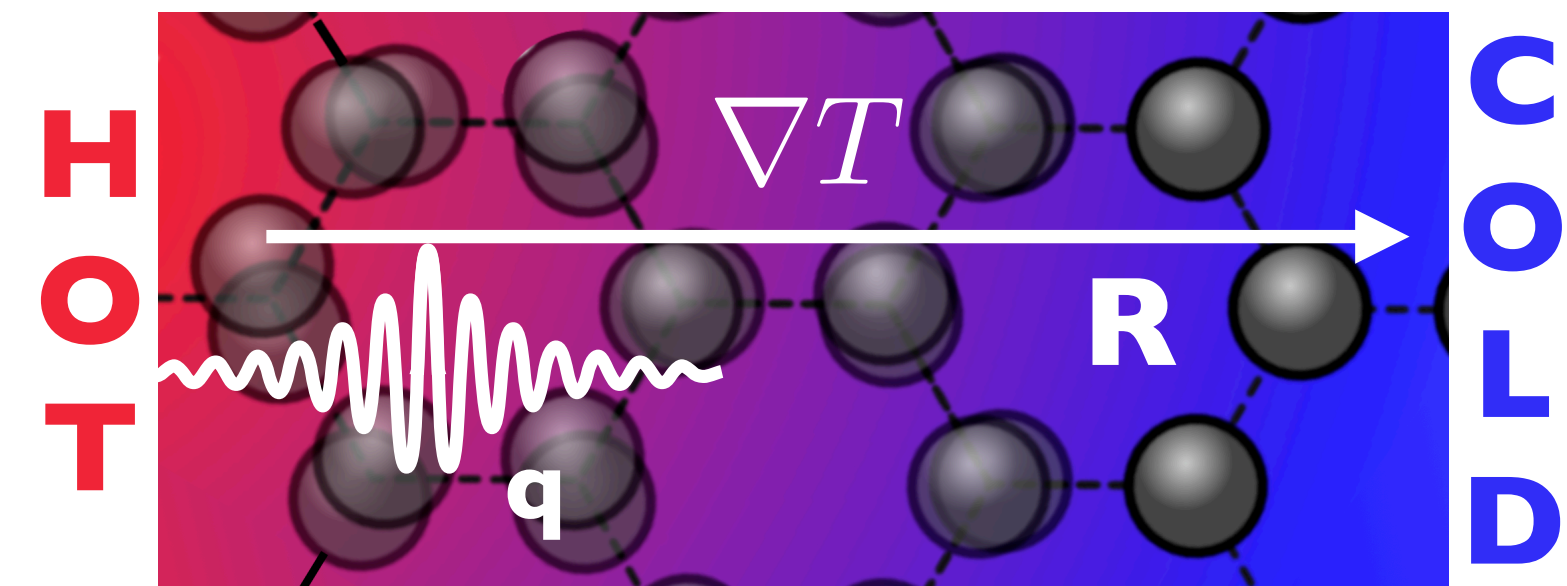
electron Wigner distribution $F(\mathbf{r}, \mathbf{k}, t)_{m,m'}$
 At equilibrium, diagonal elements = Fermi-Dirac

Electronic velocity operator (diagonal $\frac{\partial \epsilon(\mathbf{k})_m}{\partial \mathbf{k}}$) $\mathbf{V}(\mathbf{k})_{m,m'}$

$$\frac{\partial F(\mathbf{r}, \mathbf{k}, t)}{\partial t} + i[\mathcal{E}(\mathbf{k}) + \mathbf{d}(\mathbf{k}) \cdot \mathbf{E}, F(\mathbf{r}, \mathbf{k}, t)] + \frac{1}{2} \{ \mathbf{V}(\mathbf{k}), \cdot \nabla_{\mathbf{r}} F(\mathbf{r}, \mathbf{k}, t) \} - e\mathbf{E} \cdot \nabla_{\mathbf{k}} F(\mathbf{r}, \mathbf{k}, t) = \frac{\partial F(\mathbf{r}, \mathbf{k}, t)}{\partial t} \Big|_{\text{coll}}$$

lafrate, Sokolov, Krieger, *Phys. Rev. B* 96, 144303 (2017);
 Cepellotti & Kozinsky, *Materials Today Physics* 19 (2021) 100412

Wigner transport equation for phonons



$N(\mathbf{R}, \mathbf{q}, t)_{s,s'}$ phonon Wigner distribution
 At equilibrium, diagonal elements = Bose-Einstein

$\mathbf{V}(\mathbf{q})_{s,s'}$ Phonon velocity operator (diagonal $\frac{\partial \omega(\mathbf{q})_s}{\partial \mathbf{q}}$)

$$\frac{\partial \mathbf{N}(\mathbf{R}, \mathbf{q}, t)}{\partial t} + i[\mathbf{\Omega}(\mathbf{q}), \mathbf{N}(\mathbf{R}, \mathbf{q}, t)] + \frac{1}{2} \{ \vec{\mathbf{V}}(\mathbf{q}), \cdot \vec{\nabla}_{\mathbf{R}} \mathbf{N}(\mathbf{R}, \mathbf{q}, t) \} = \frac{\partial \mathbf{N}(\mathbf{R}, \mathbf{q}, t)}{\partial t} \Big|_{\text{Hcol}}$$

Simoncelli, Marzari and Mauri, *Nat. Phys.* 15 (2019)
 Simoncelli, Marzari and Mauri, *Phys. Rev. X* 12 (2022)

coherences
 populations

couplings
 Group velocity

WIGNER CONDUCTIVITIES FOR ELECTRONS AND PHONONS

linear response in ∇T of phonon Wigner equation yields the heat flux \mathbf{Q} , thus thermal conductivity ($\mathbf{Q} = -\kappa \nabla T$)

$$\kappa^{\alpha\beta} = \kappa_P^{\alpha\beta} + \frac{1}{VN_q} \sum_{\mathbf{q}, s \neq s'} \frac{\omega(\mathbf{q})_s + \omega(\mathbf{q})_{s'}}{4} \left[\frac{C(\mathbf{q})_s}{\omega(\mathbf{q})_s} + \frac{C(\mathbf{q})_{s'}}{\omega(\mathbf{q})_{s'}} \right] v^\alpha(\mathbf{q})_{s,s'} v^\beta(\mathbf{q})_{s',s} \frac{\frac{1}{2} [\Gamma(\mathbf{q})_s + \Gamma(\mathbf{q})_{s'}]}{[\omega(\mathbf{q})_{s'} - \omega(\mathbf{q})_s]^2 + \frac{1}{4} [\Gamma(\mathbf{q})_s + \Gamma(\mathbf{q})_{s'}]^2}$$

Simoncelli, Marzari and Mauri, Nat. Phys. 15 (2019)

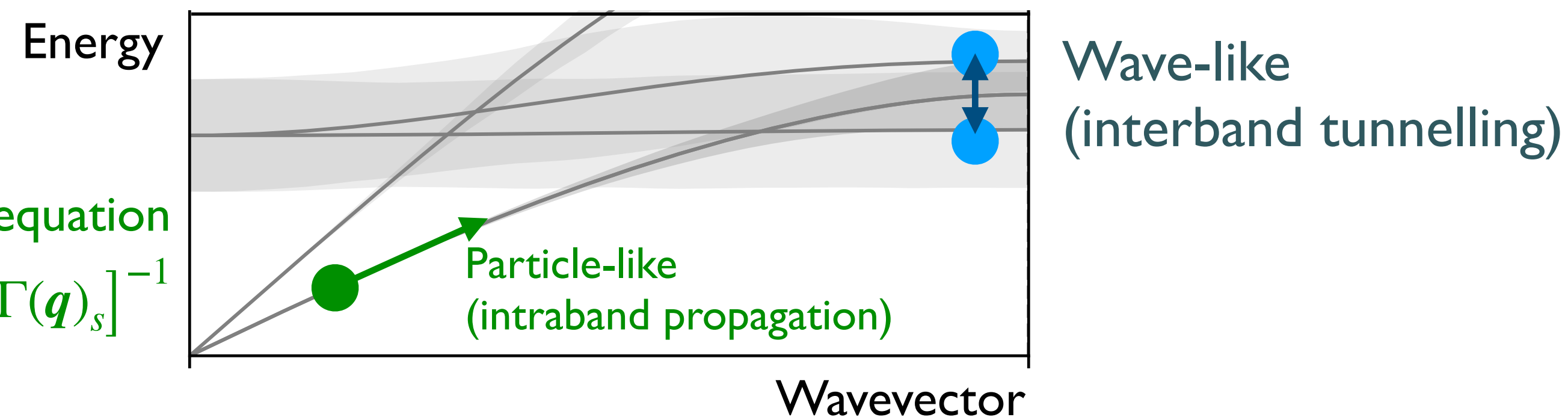
linear response in \mathbf{E} of electron Wigner equation yields the charge current \mathbf{J} , thus electrical conductivity $\mathbf{J} = -\sigma \mathbf{E}$

$$\sigma^{\alpha\beta} = \sigma_P^{\alpha\beta} + \frac{g_s}{VN_k} \sum_{\mathbf{k}, m \neq m'} \frac{f(\mathbf{k}')_{m'} - f(\mathbf{k})_m}{\epsilon(\mathbf{k}')_{m'} - \epsilon(\mathbf{k})_m} v^\alpha(\mathbf{k})_{m,m'} v^\beta(\mathbf{k})_{m',m} \frac{\frac{1}{2} [\Gamma(\mathbf{k})_m + \Gamma(\mathbf{k})_{m'}]}{[\epsilon(\mathbf{k})_{m'} - \epsilon(\mathbf{k})_m]^2 + \frac{1}{4} [\Gamma(\mathbf{k})_m + \Gamma(\mathbf{k})_{m'}]^2}$$

Cepellotti and Kozinsky, Materials Today Physics 19 (2021)

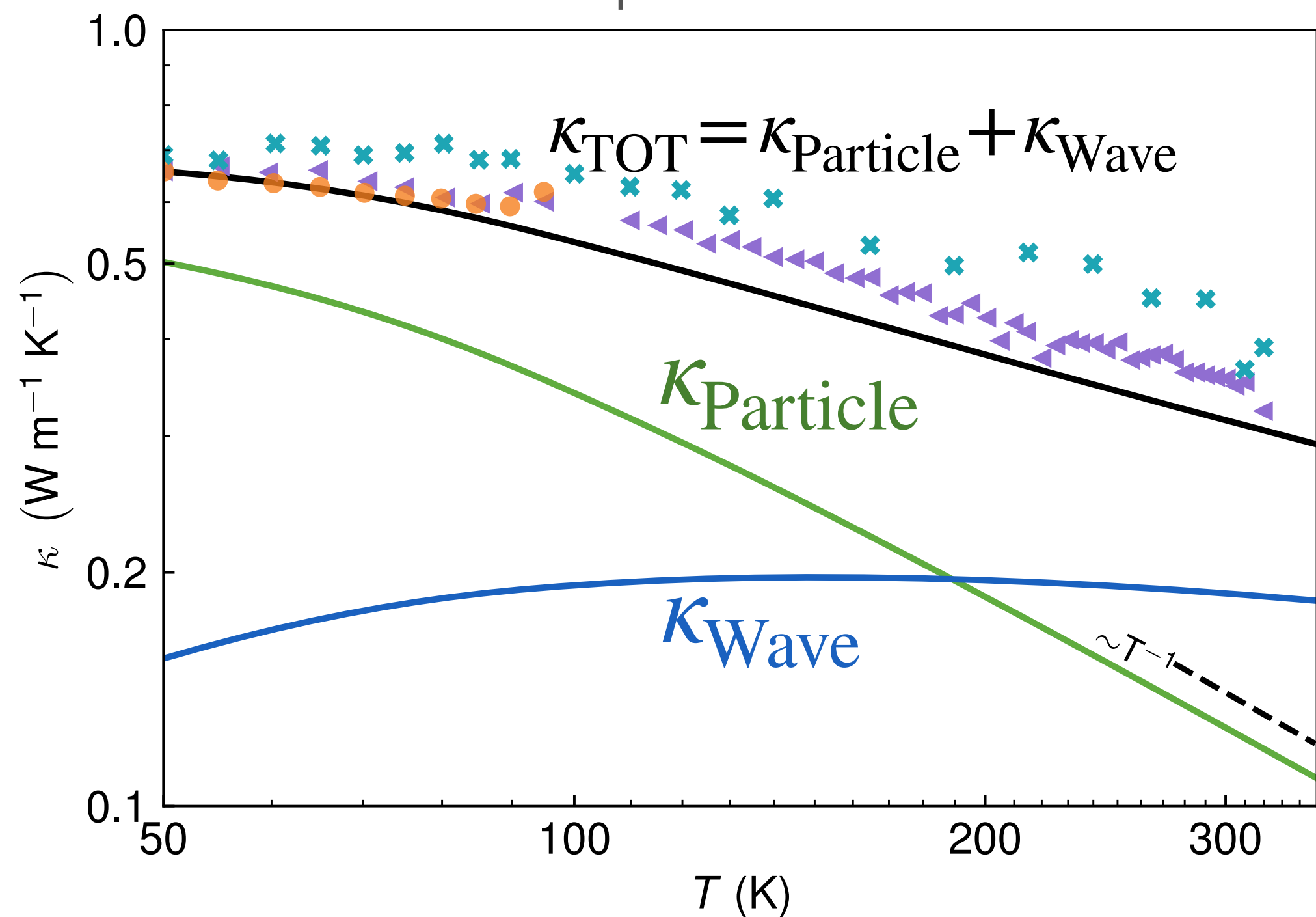
Equivalent to Boltzmann transport equation

$$\kappa_P \sim \frac{1}{3VN_q} \sum_{\mathbf{q}, s} C(\mathbf{q})_s v^2(\mathbf{q})_s [\Gamma(\mathbf{q})_s]^{-1}$$



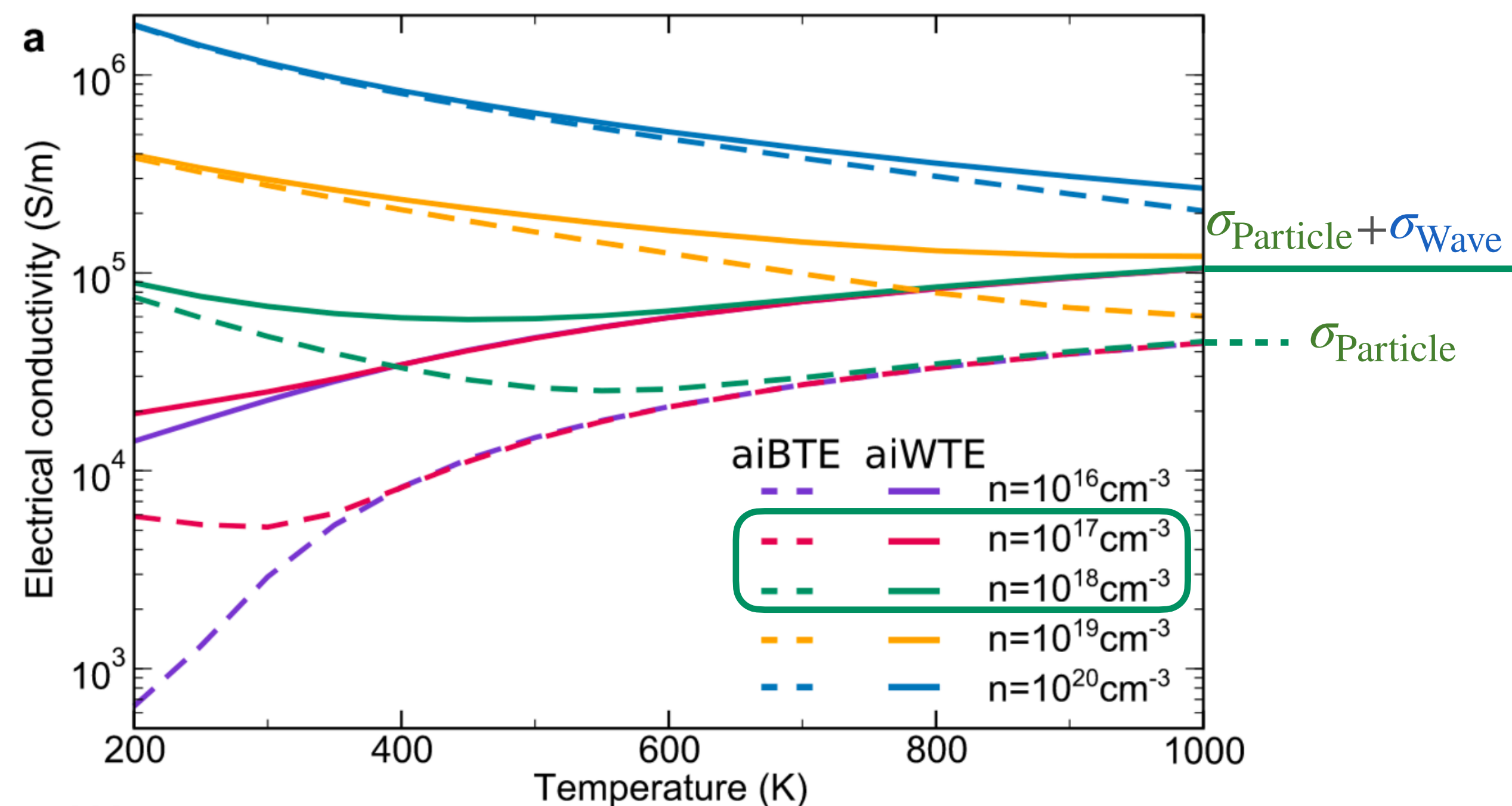
DUAL WAVE-PARTICLE TRANSPORT

Phonon transport in CsPbBr₃



Simoncelli, Marzari, Mauri, Nat. Phys. 15 (2019)

Electron transport in Bi₂Se₃



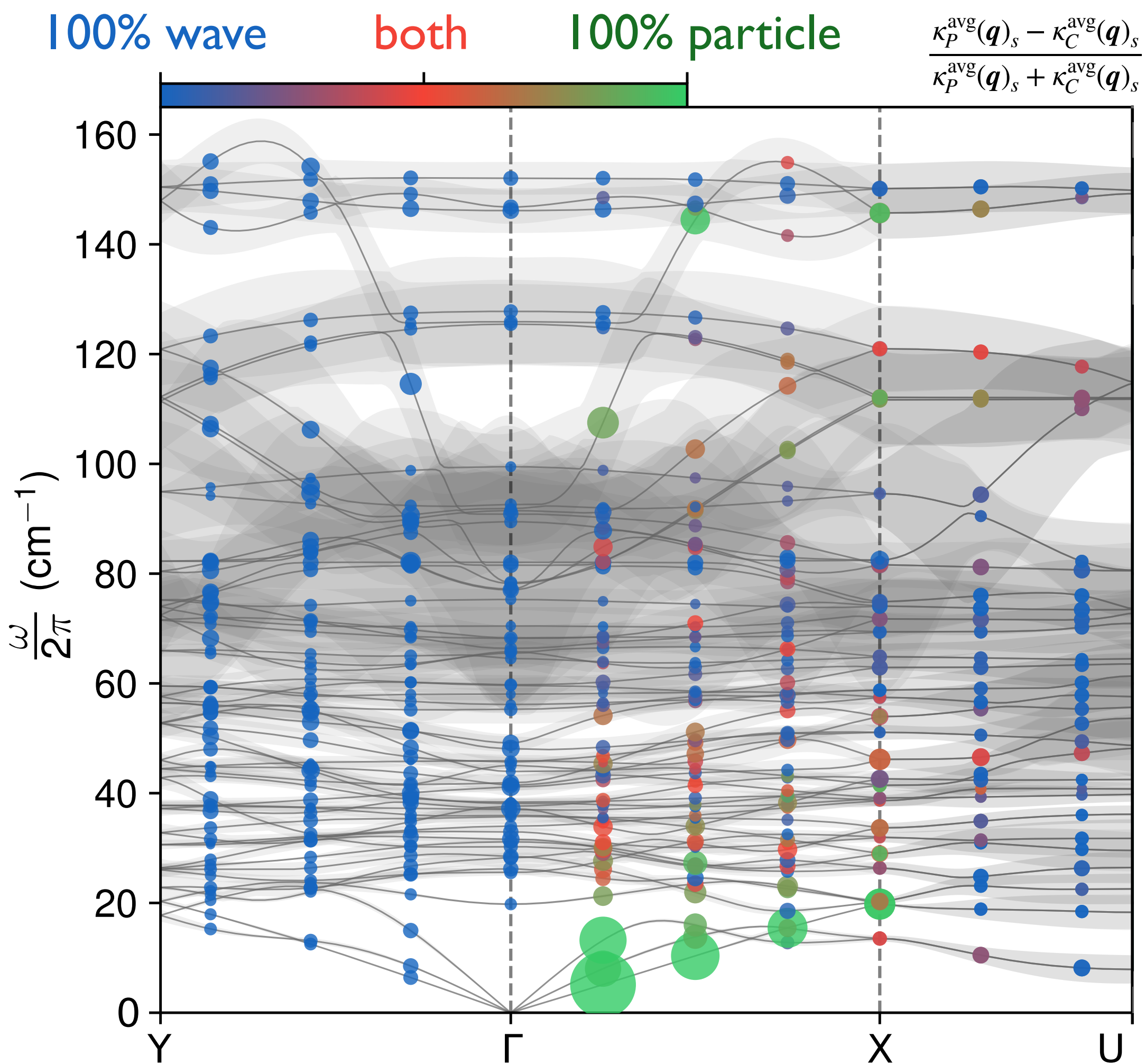
Cepellotti and Kozinsky, Materials Today Physics 19 (2021)



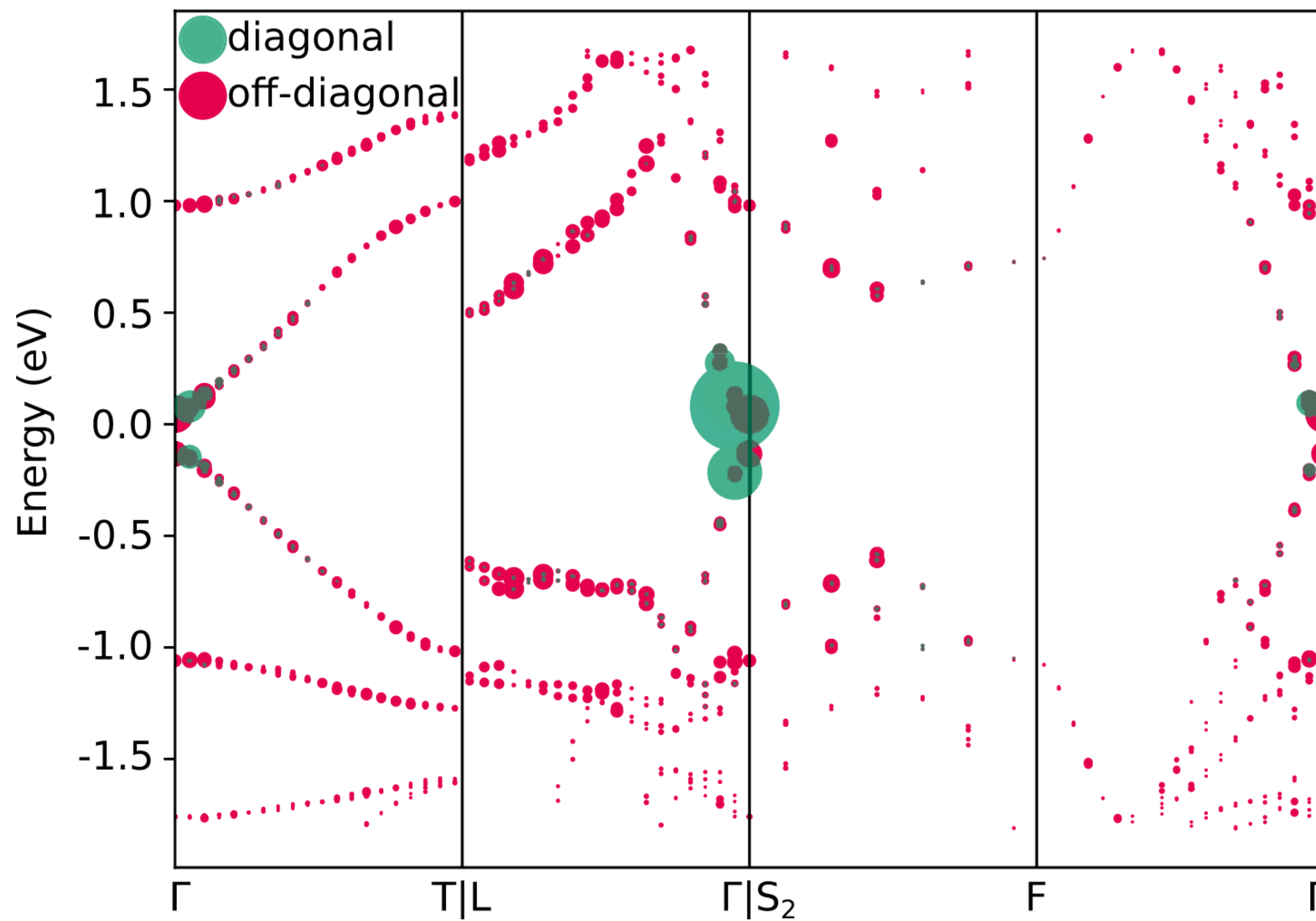
DUAL WAVE-PARTICLE TRANSPORT

Phonon transport in CsPbBr₃

Electron transport in Bi₂Se₃



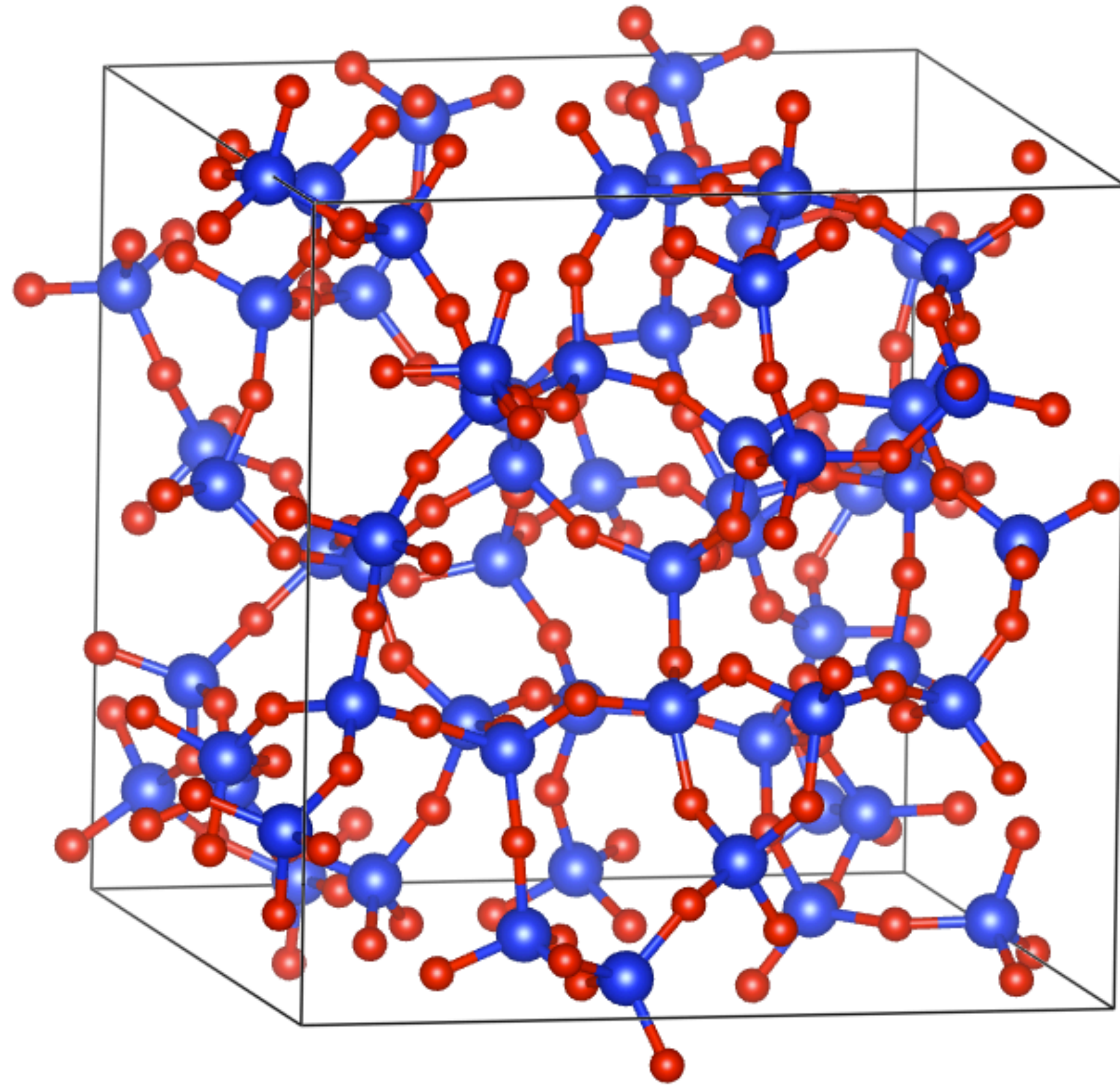
Simoncelli, Marzari, Mauri, Nat. Phys. 15 (2019)



Cepellotti and Kozinsky, Materials Today Physics 19 (2021)

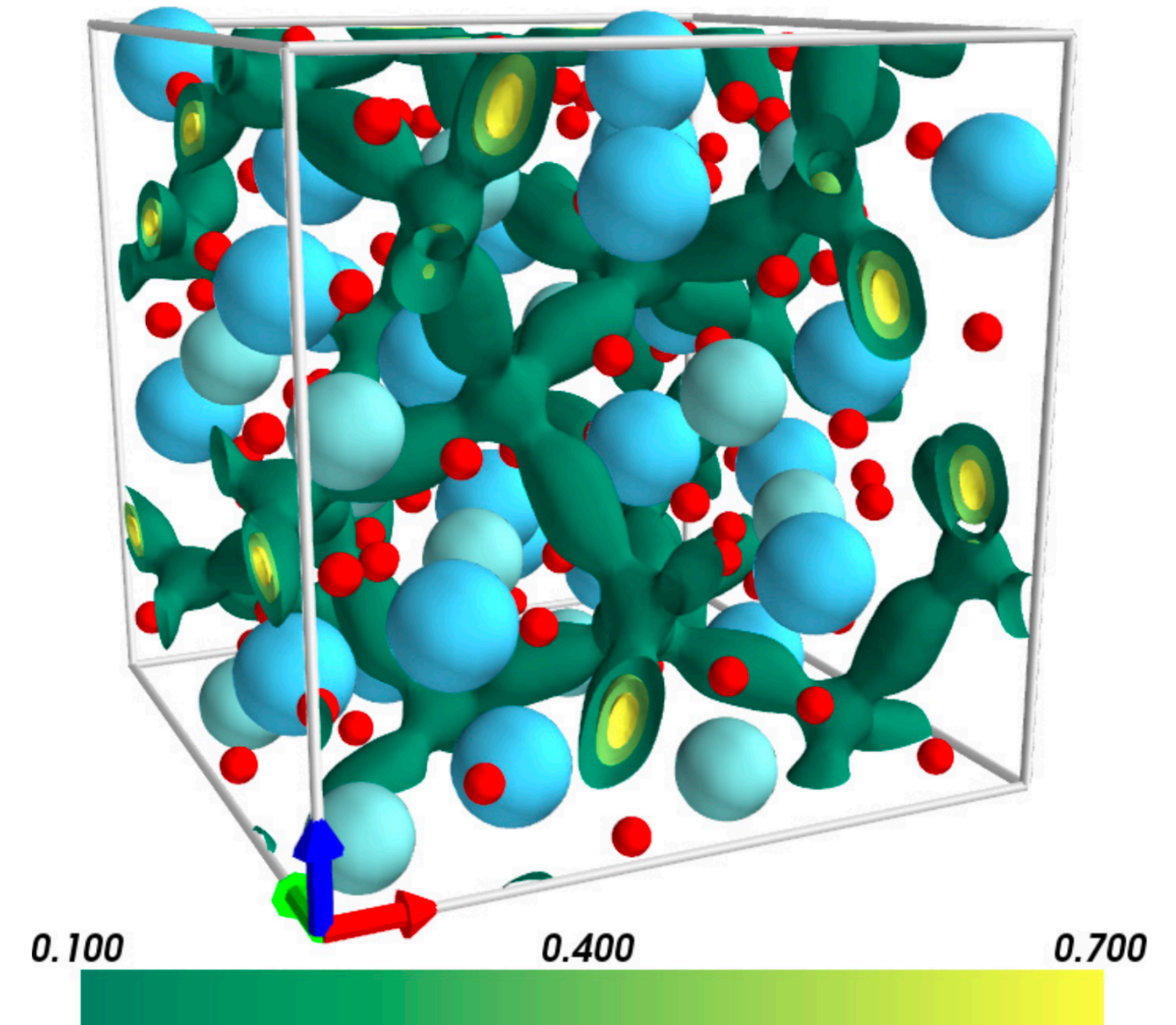
BEYOND BAND TRANSPORT

Heat transfer in amorphous solids



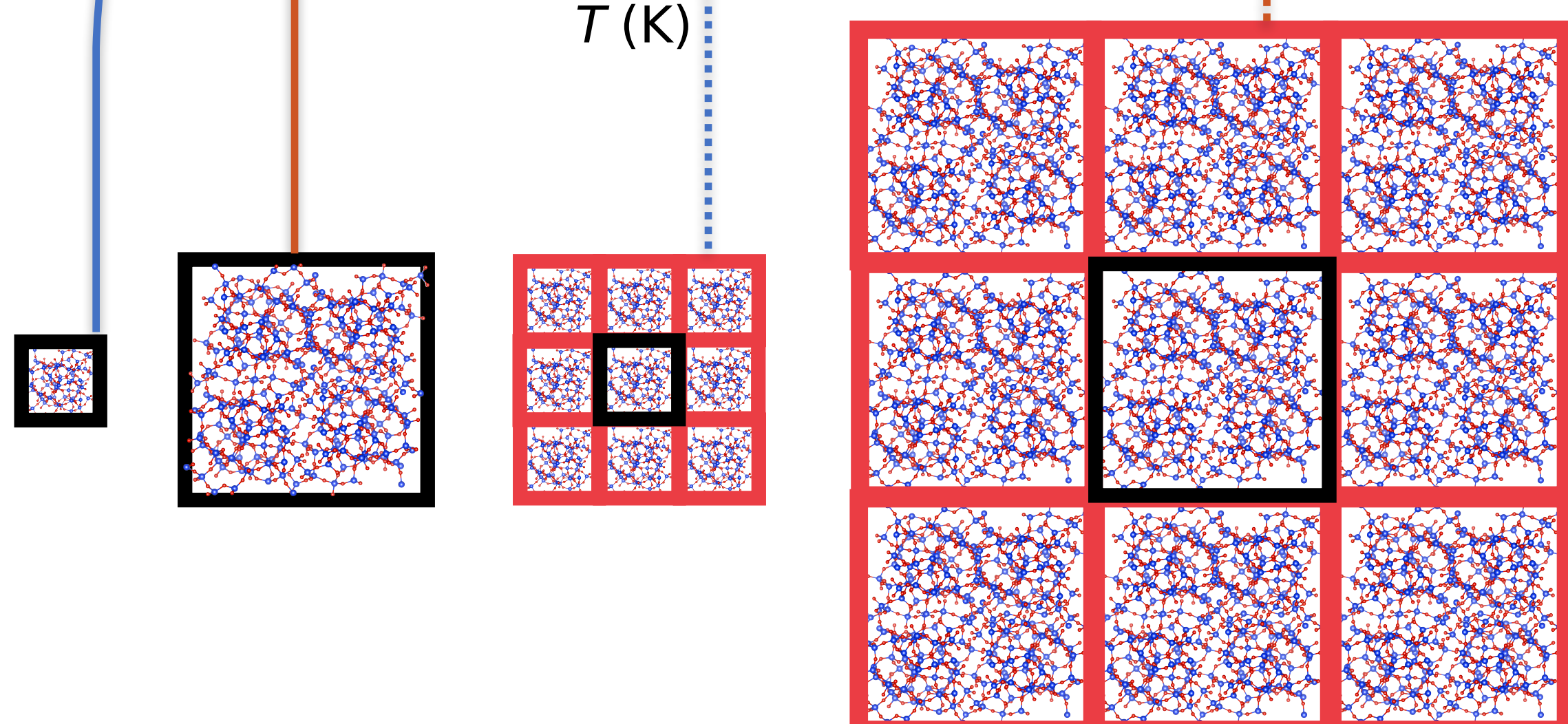
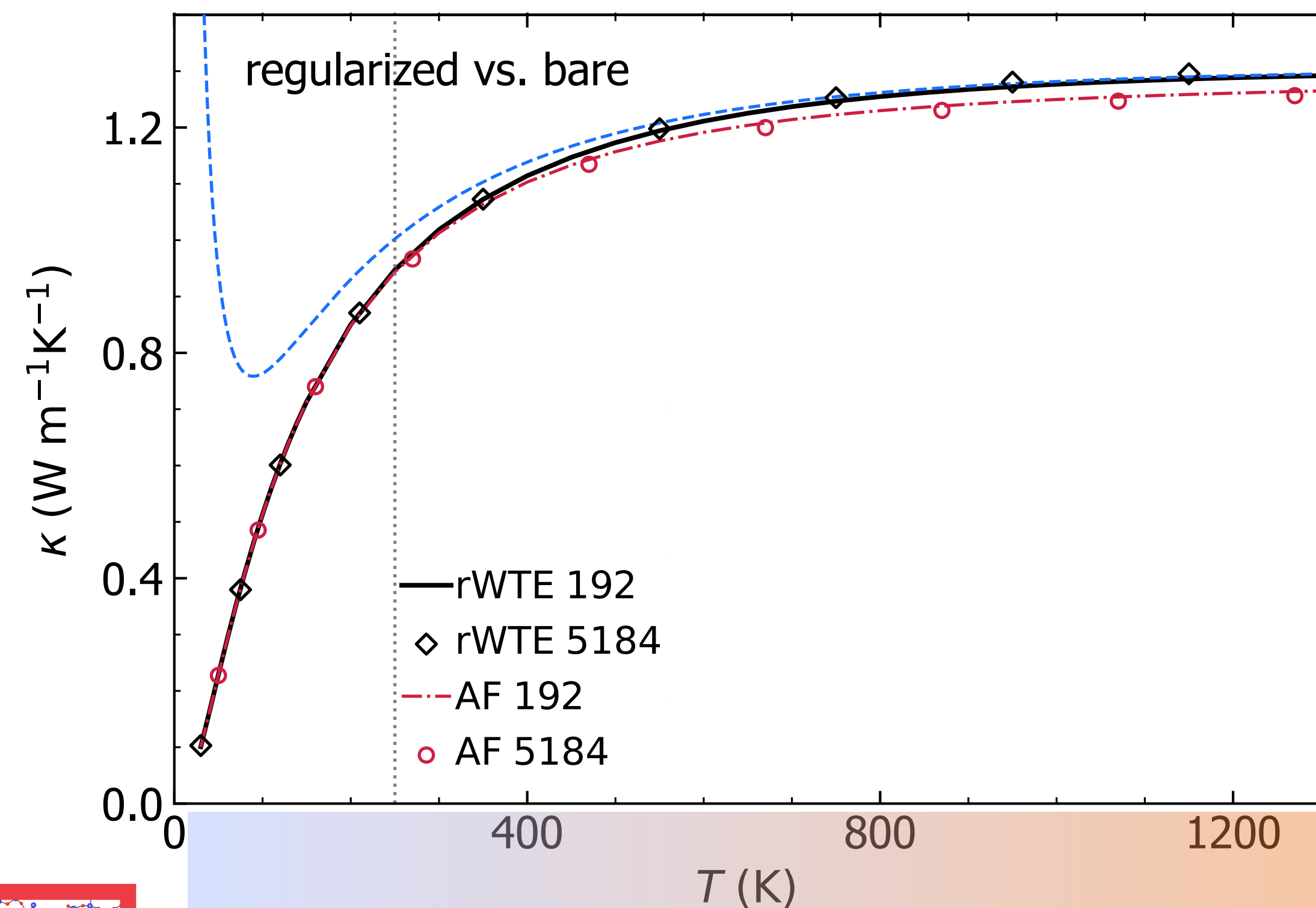
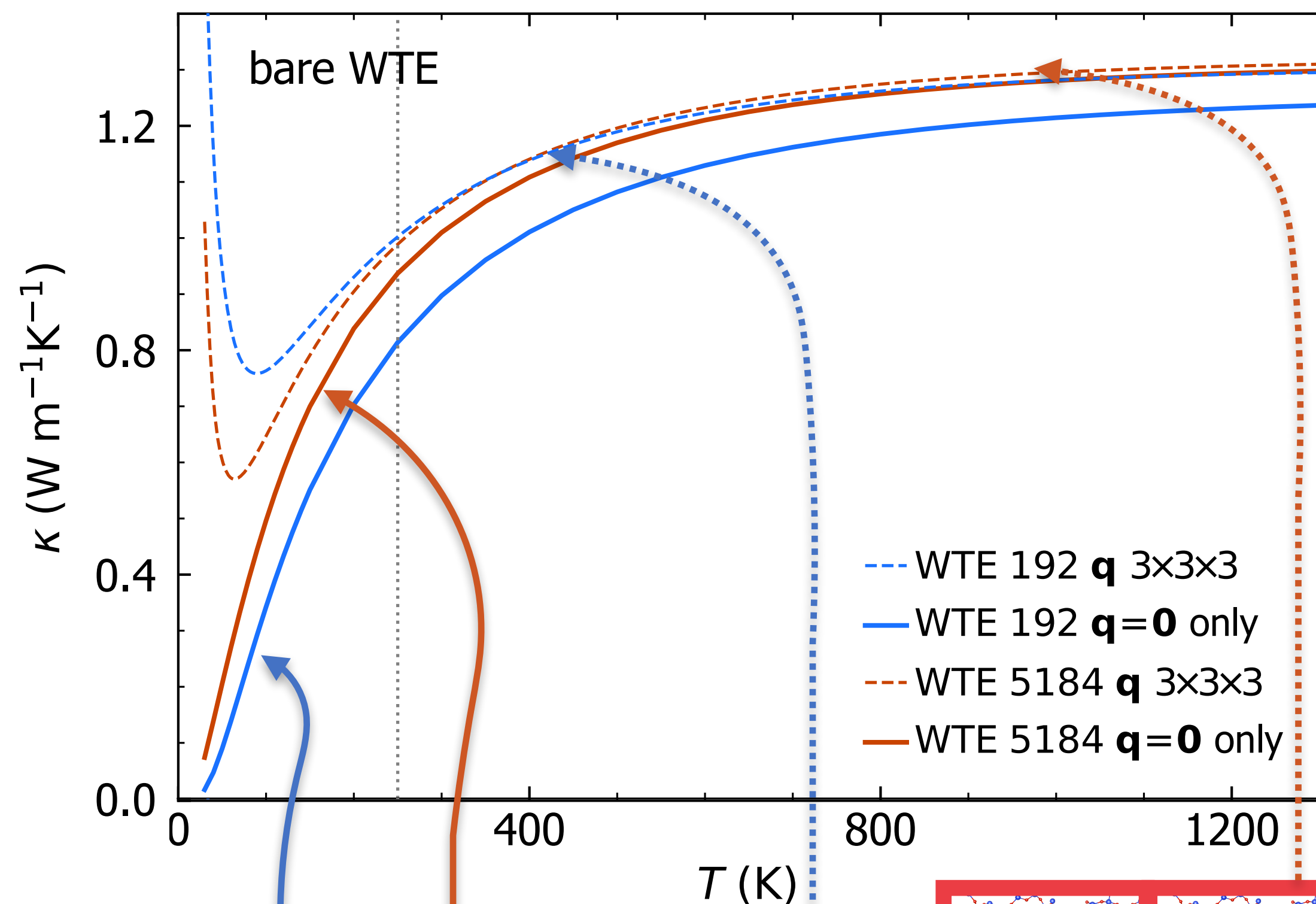
Atomistic model of SiO₂ generated from first principles
Simoncelli, Mauri, Marzari, npj Comput. Mater. 9 (2023);

Charge transfer in solid-state ionic conductors



Li-ion percolation pathways in Li₇La₃Zr₂O₁₂
Kahle et al., Phys. Rev. Materials 3, 055404 (2019)

PROTOCOL FOR HEAT TRANSPORT IN GLASSES



$$\frac{1}{\sqrt{2\pi\eta}} e^{-\frac{(\omega(\mathbf{q})_s - \omega(\mathbf{q})_{s'})^2}{2\eta^2}}$$

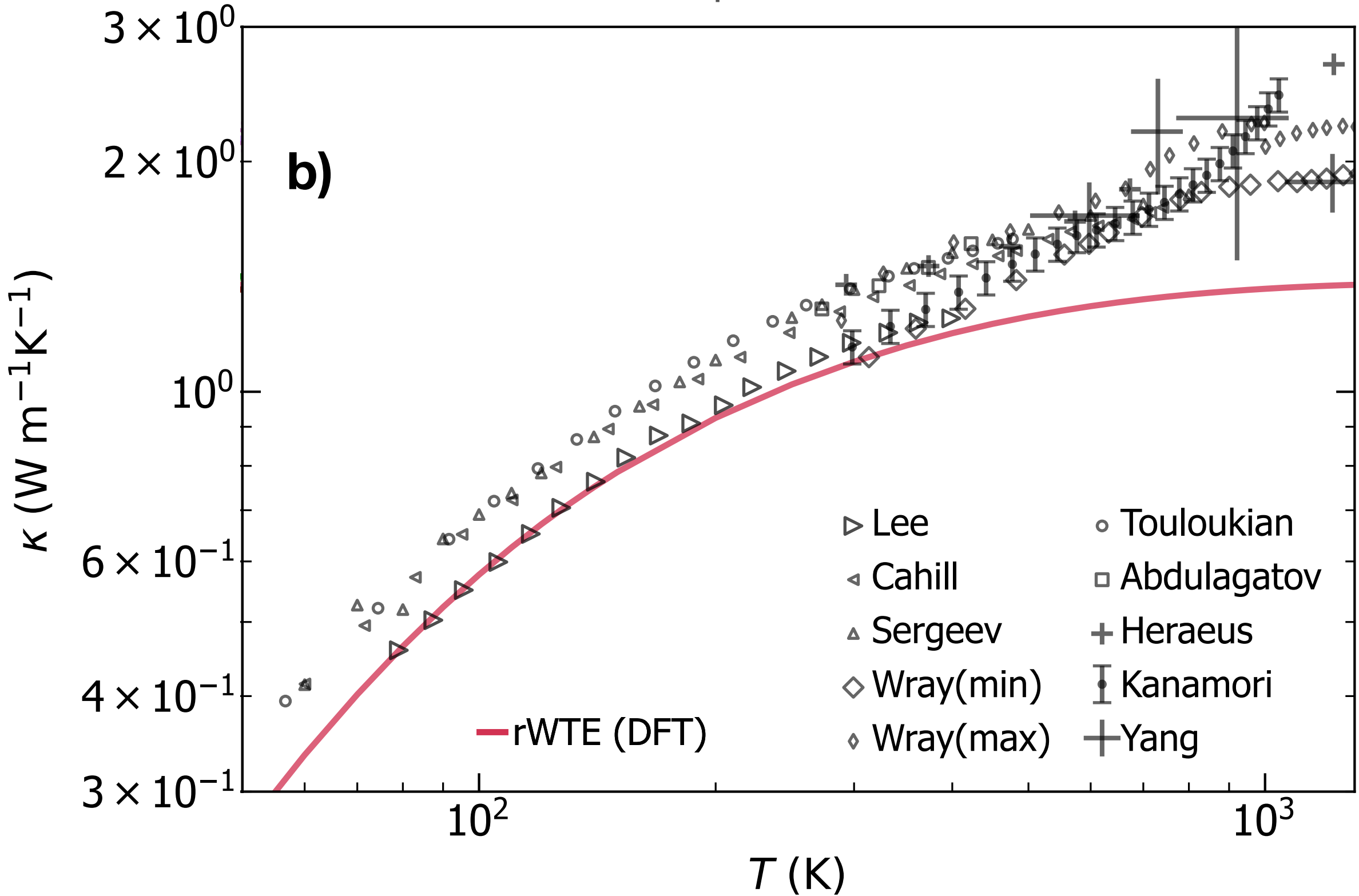
$$\frac{1}{\pi} \frac{\frac{1}{2}(\Gamma(\mathbf{q})_s + \Gamma(\mathbf{q})_{s'})}{(\omega(\mathbf{q})_s - \omega(\mathbf{q})_{s'})^2 + \frac{1}{4}(\Gamma(\mathbf{q})_s + \Gamma(\mathbf{q})_{s'})^2}}$$

Voigt profile $\mathcal{F}_{[\eta; \Gamma(\mathbf{q})_s + \Gamma(\mathbf{q})_{s'}]}(\omega(\mathbf{q})_s - \omega(\mathbf{q})_{s'})$

$\Gamma(\mathbf{q})_s \ll \eta$ $\Gamma(\mathbf{q})_s \gg \eta$

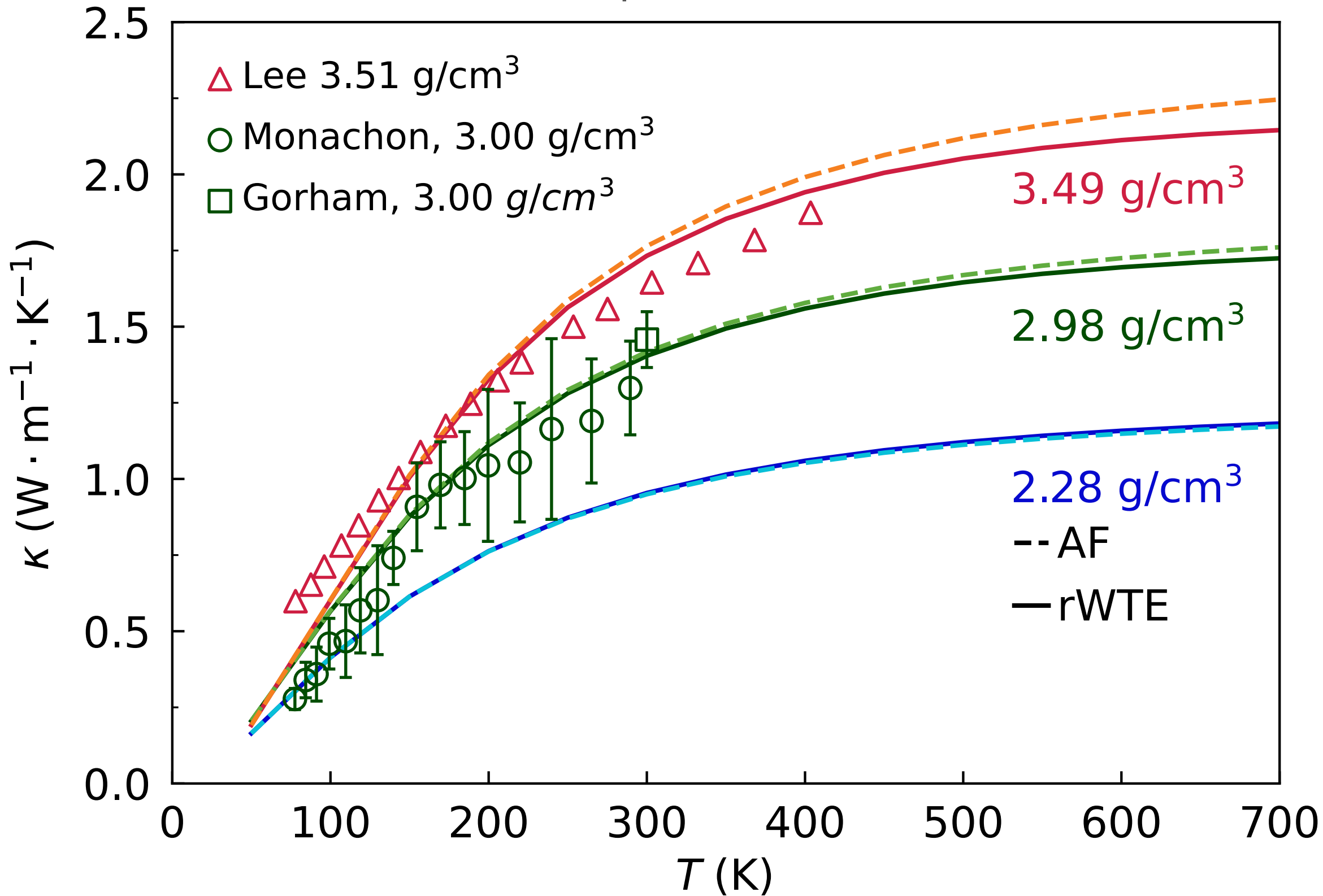
CONDUCTIVITY OF GLASSES FROM FIRST PRINCIPLES

Amorphous SiO₂



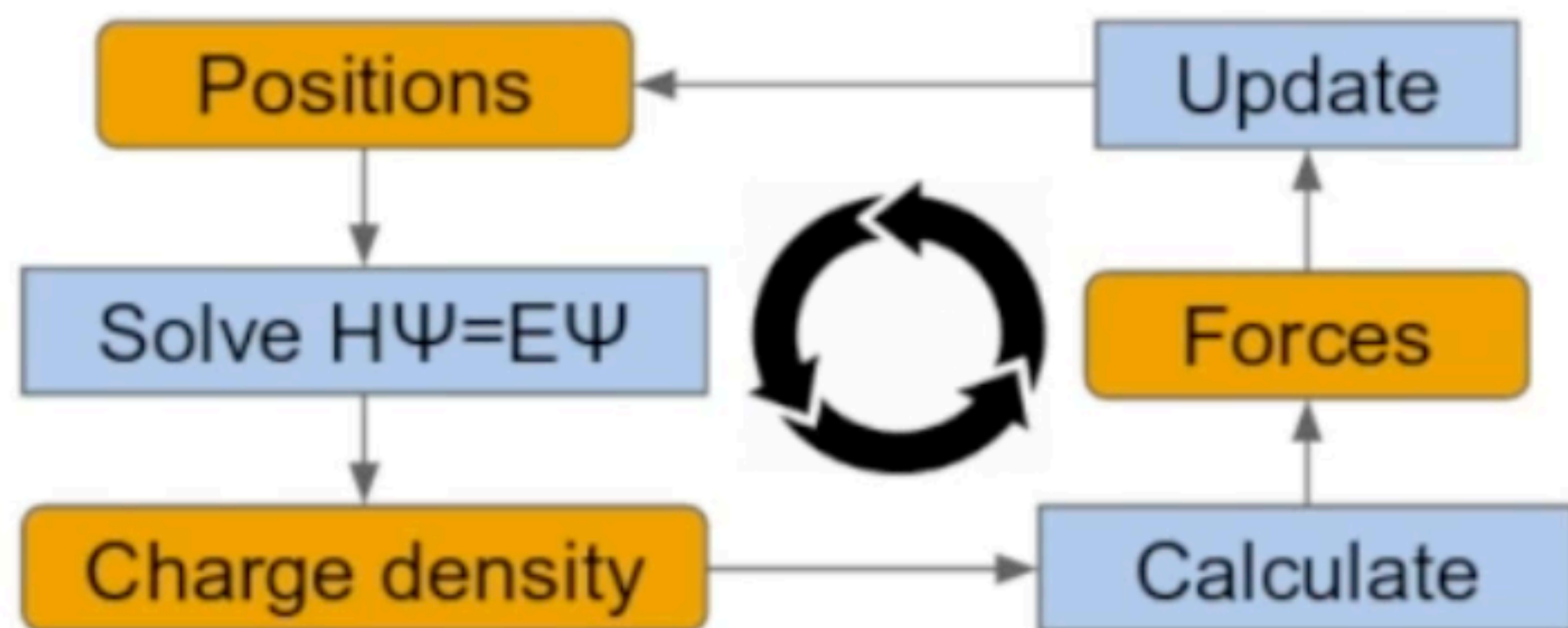
Simoncelli, Mauri, Marzari, *npj Comput. Mater.* 9 (2023)

Amorphous Al₂O₃

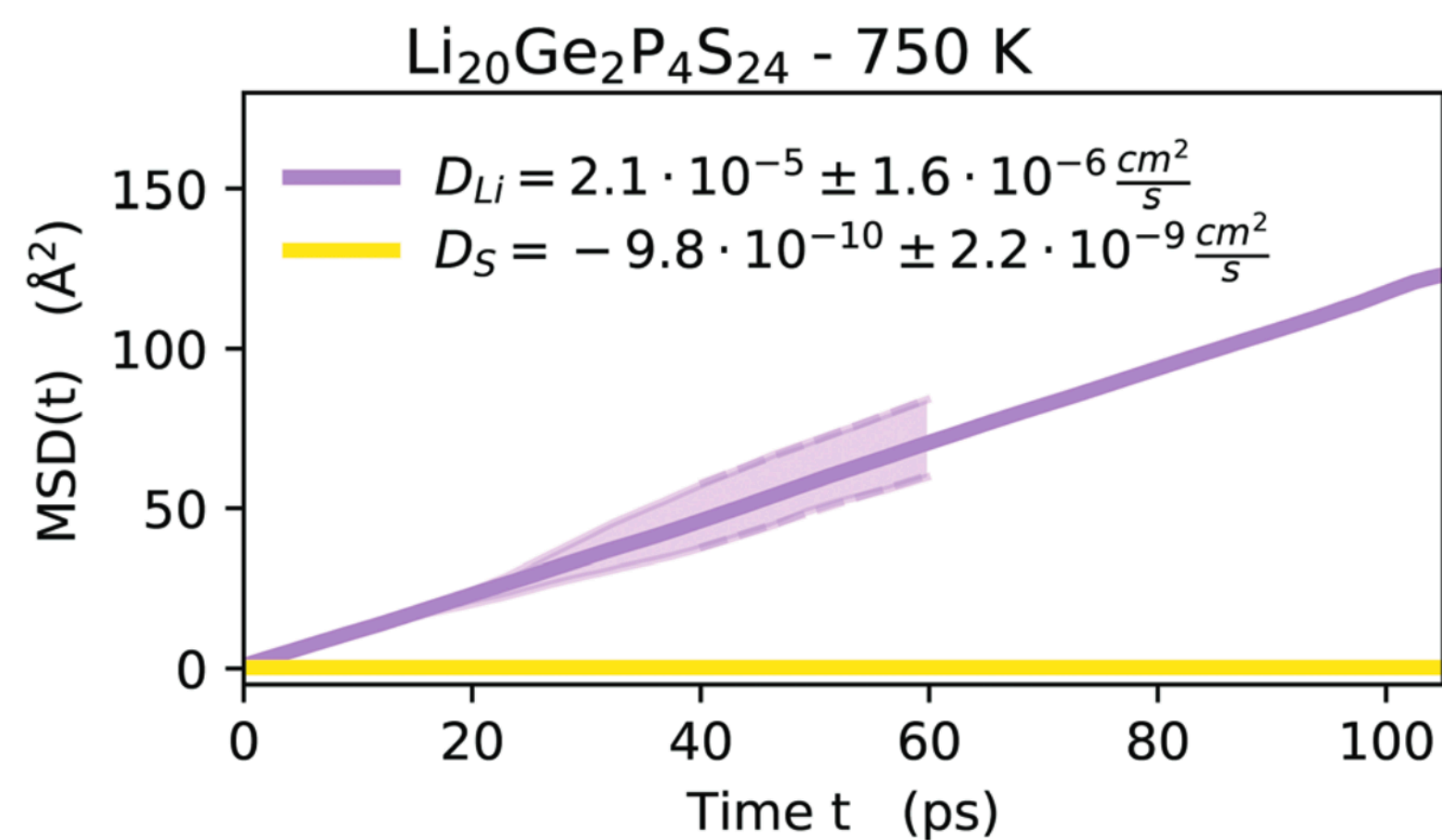


Harper, Iwanowski, Payne, Simoncelli *arXiv 2303.08637* (2023)

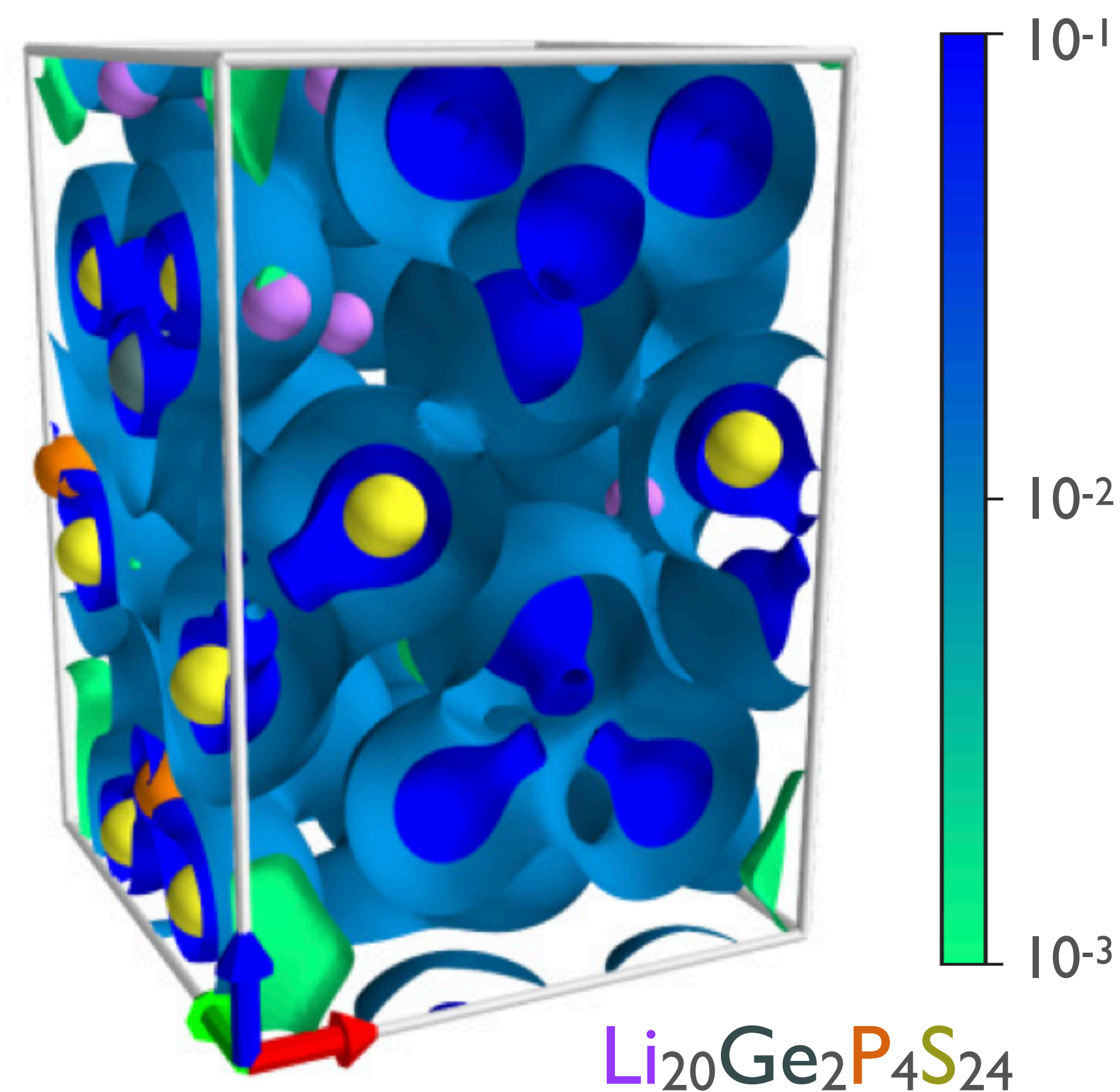
IONIC DIFFUSIVITY FROM AB INITIO MOLECULAR DYNAMICS



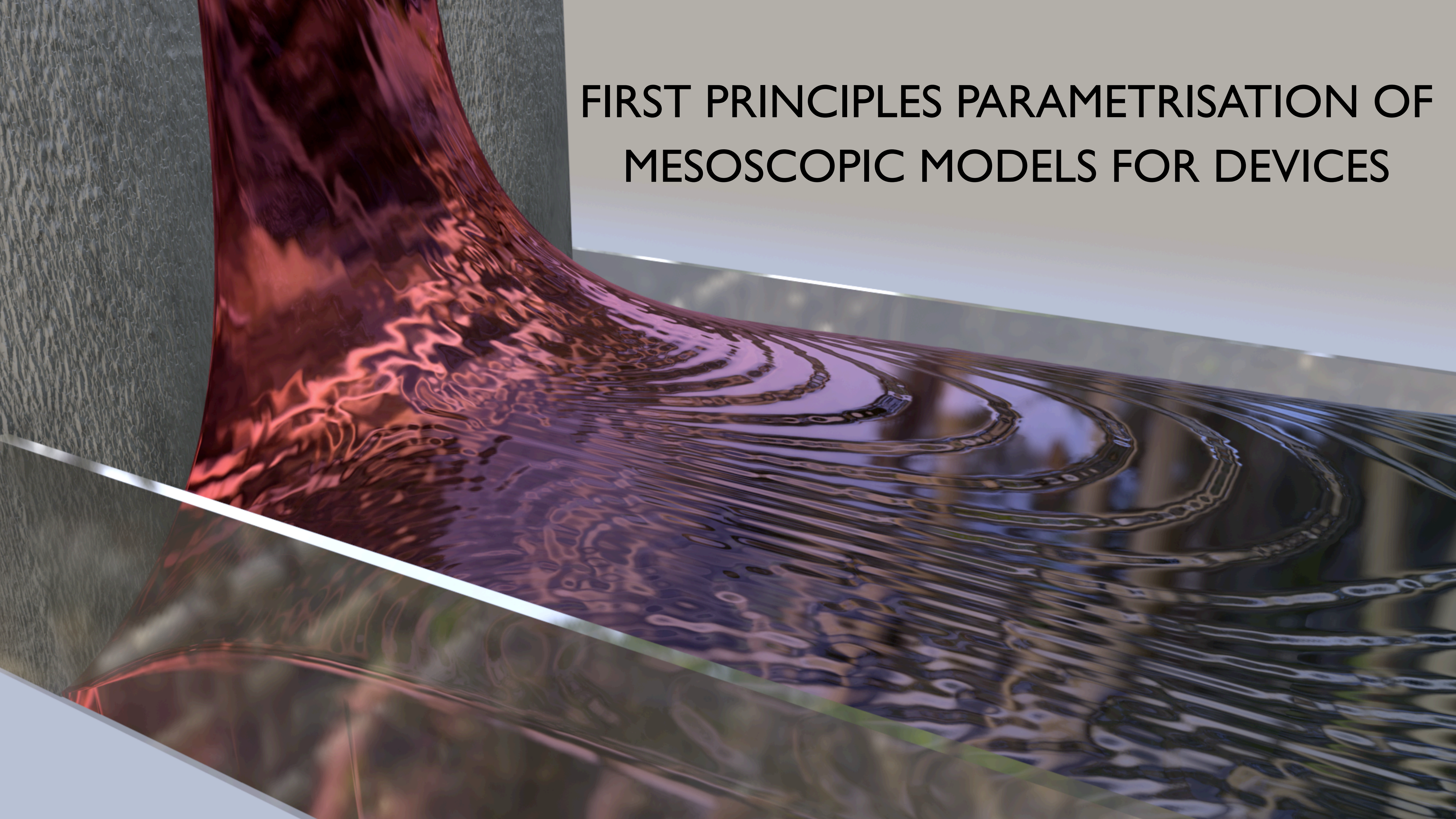
Ionic conductors:
$$D_{\text{tr}}^{\text{Li}} = \lim_{t \rightarrow \infty} \frac{1}{6t} \frac{1}{N_{\text{Li}}} \sum_l^{\text{Li}} \langle |\mathbf{R}_l(t + \tau) - \mathbf{R}_l(\tau)|^2 \rangle_\tau$$



Isosurfaces of valence electronic charge density

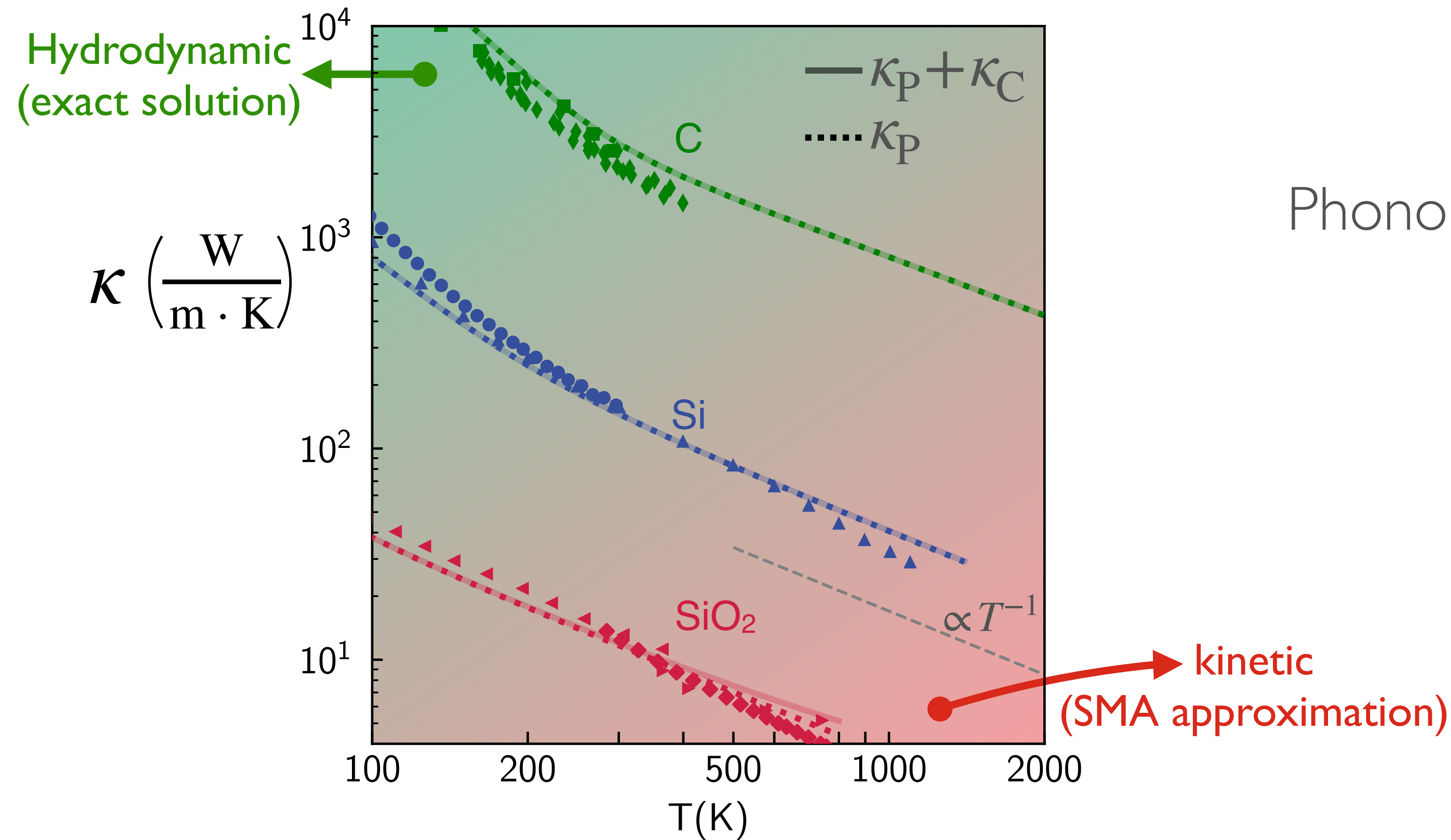


Kahle, Marcolongo, & Marzari, *Phys. Rev. Materials* 2 (2018)
 Kahle, Marcolongo, & Marzari, *Energy Environ. Sci.* 13 (2020)

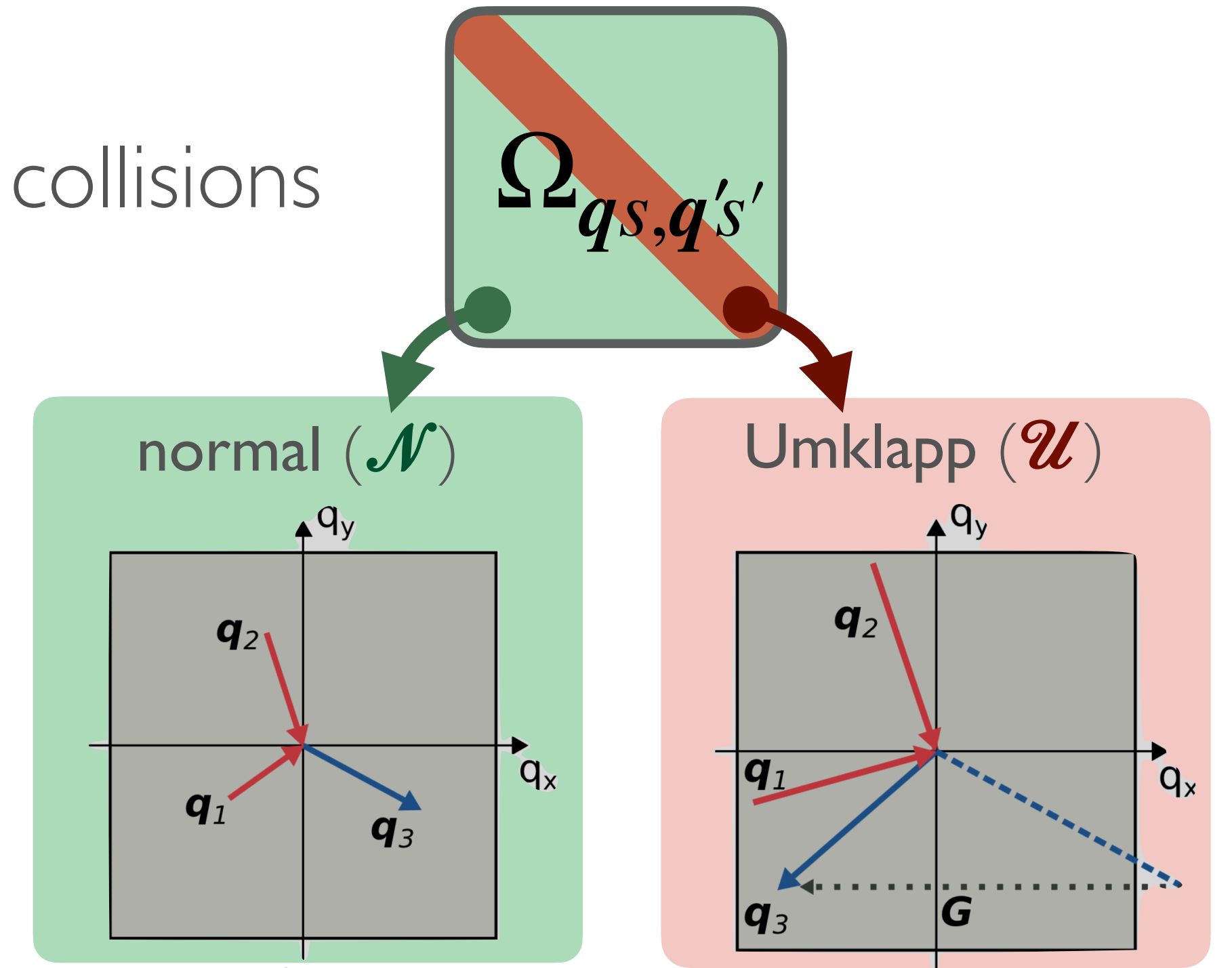
A 3D rendered scene showing a thick stream of red liquid pouring from the top left onto a highly reflective, metallic surface. The liquid spreads out, creating a series of concentric ripples and reflections that catch the light, giving it a shimmering, almost iridescent appearance. The background is a plain, light-colored wall and floor, which also reflect the scene.

FIRST PRINCIPLES PARAMETRISATION OF MESOSCOPIC MODELS FOR DEVICES

HEAT HYDRODYNAMICS IN SIMPLE CRYSTALS WITH $\kappa_P \gg \kappa_C$



Phonon collisions



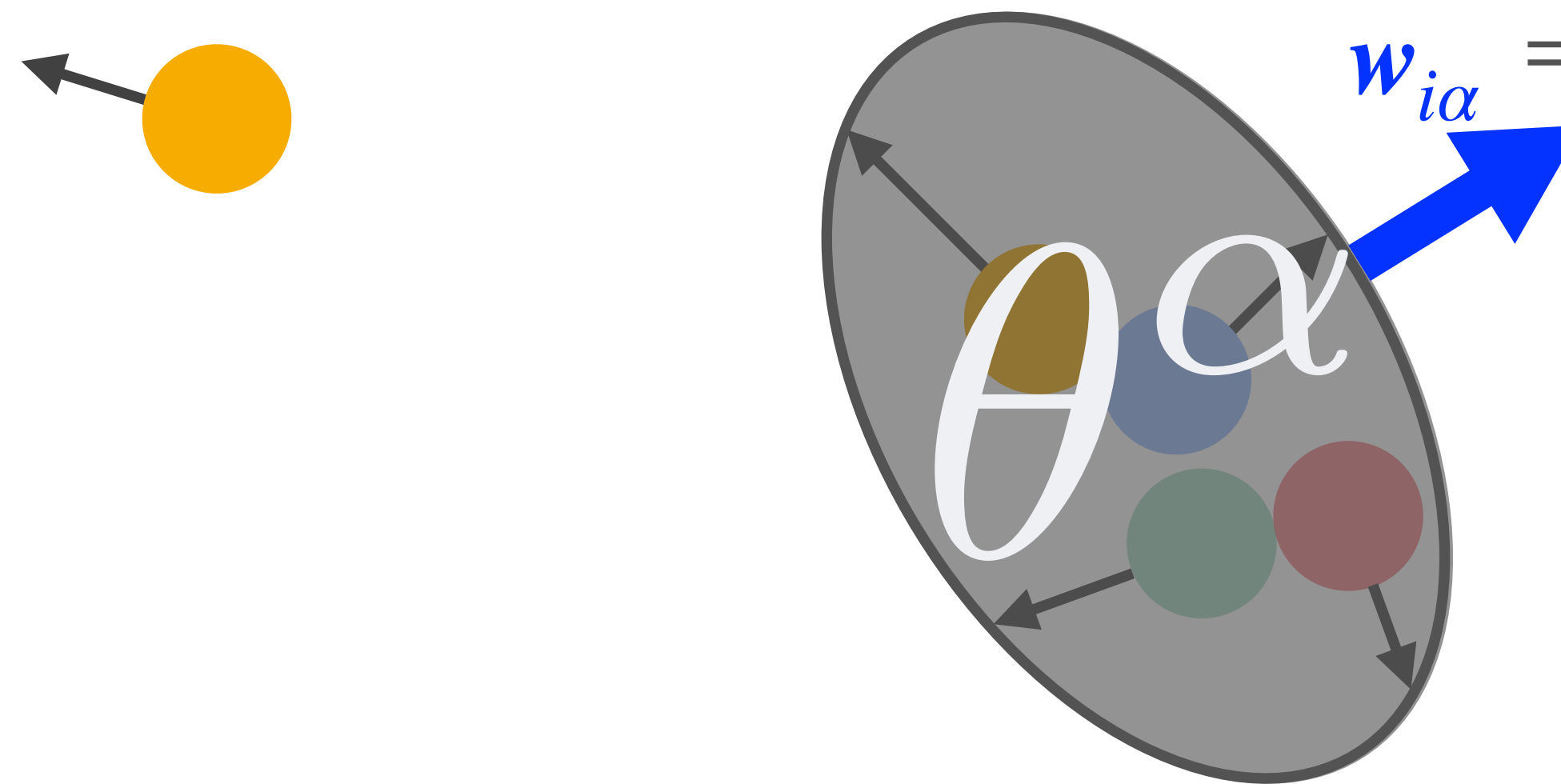
Particle-like conduction dominates, Peierls-Boltzmann equation is accurate

$$\frac{\partial N(\mathbf{x}, \mathbf{q}, t)_s}{\partial t} + \vec{V}(\mathbf{q})_s \cdot \nabla_{\mathbf{x}} N(\mathbf{x}, \mathbf{q}, t)_s = - \sum_{\mathbf{q}'s'} \Omega_{qs, \mathbf{q}'s'} [N(\mathbf{x}, \mathbf{q}', t)_{s'} - \bar{N}(\mathbf{q}')_{s'}]$$

RELAXONS: EXACT SOLUTION & MICROSCOPIC INSIGHTS

How to define heat carriers and relaxation time in the hydrodynamic regime?

$$\frac{\partial N(\mathbf{x}, \mathbf{q}, t)_s}{\partial t} + \vec{V}(\mathbf{q})_s \cdot \nabla_{\mathbf{x}} N(\mathbf{x}, \mathbf{q}, t)_s = - \sum_{\mathbf{q}'s'} \Omega_{\mathbf{q}s, \mathbf{q}'s'} [N(\mathbf{x}, \mathbf{q}', t)_{s'} - \bar{N}(\mathbf{q}')_{s'}]$$



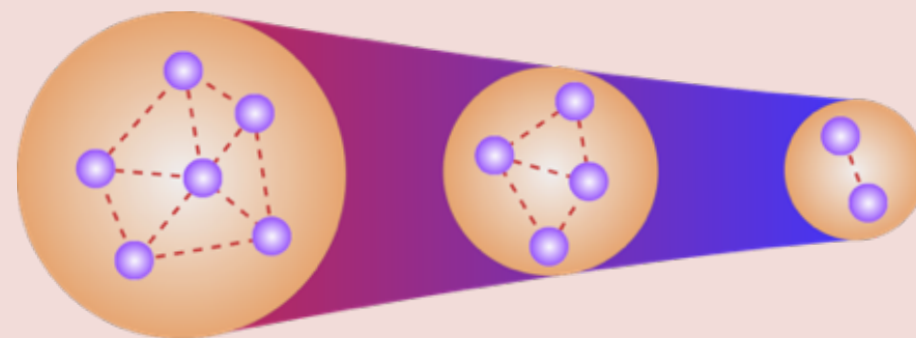
$w_{i\alpha} \Rightarrow$ Symmetrise and diagonalise the scattering matrix

$$- \sum_{\mathbf{q}'s'} \tilde{\Omega}_{\mathbf{q}s, \mathbf{q}'s'} \left| \theta(\mathbf{q}')_{s'}^\alpha \right\rangle = - \frac{1}{\tau_\alpha} \left| \theta(\mathbf{q})_s^\alpha \right\rangle$$

Relaxon $\left| \theta(\mathbf{q})_s^\alpha \right\rangle =$ cloud of interacting phonons having:

1) Exact lifetime: τ_α

relaxon
phonon



2) Velocity:

$$w_{i\alpha} = \frac{1}{V} \sum_{\mathbf{q}, s} \langle \phi(\mathbf{q})_s^i \left| V(\mathbf{q})_s \right| \theta(\mathbf{q})_s^\alpha \rangle$$

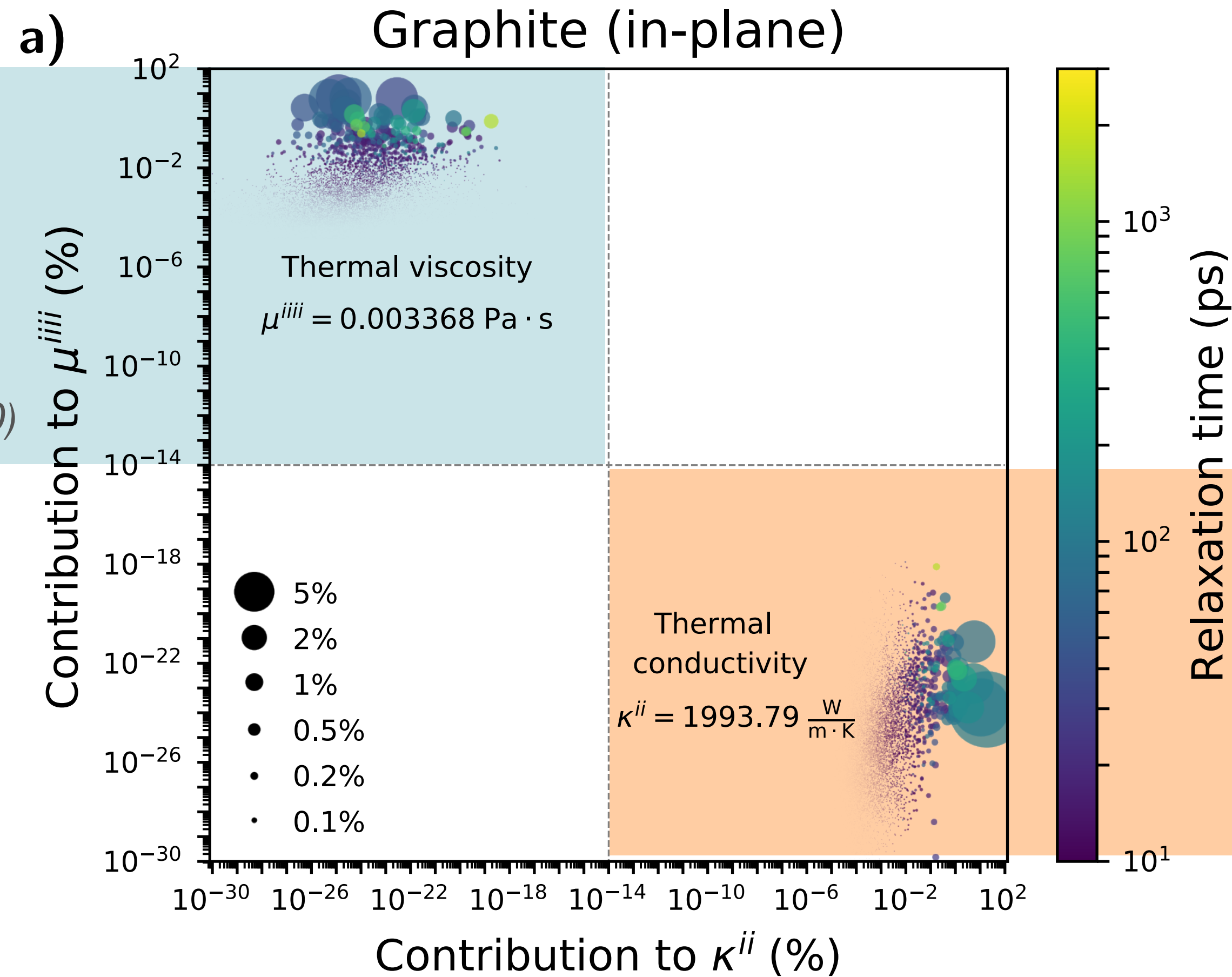
ODD & EVEN RELAXONS: CONDUCTIVITY & VISCOSITY

Relaxons have parity: even $|\theta(-\mathbf{q})_s^\alpha\rangle = + |\theta(\mathbf{q})_s^\alpha\rangle$ or odd $|\theta(-\mathbf{q})_s^\beta\rangle = - |\theta(\mathbf{q})_s^\beta\rangle$

Even relaxons $\rightarrow \mu$

$$\mu^{ijkl} = \sqrt{A^i A^k} \sum_{\alpha>0} \frac{w_{i\alpha}^j w_{k\alpha}^l + w_{i\alpha}^l w_{k\alpha}^j}{2} \tau_\alpha$$

Simoncelli, Marzari, & Cepellotti, PRX 10 (2020)



Odd relaxons $\rightarrow \kappa$

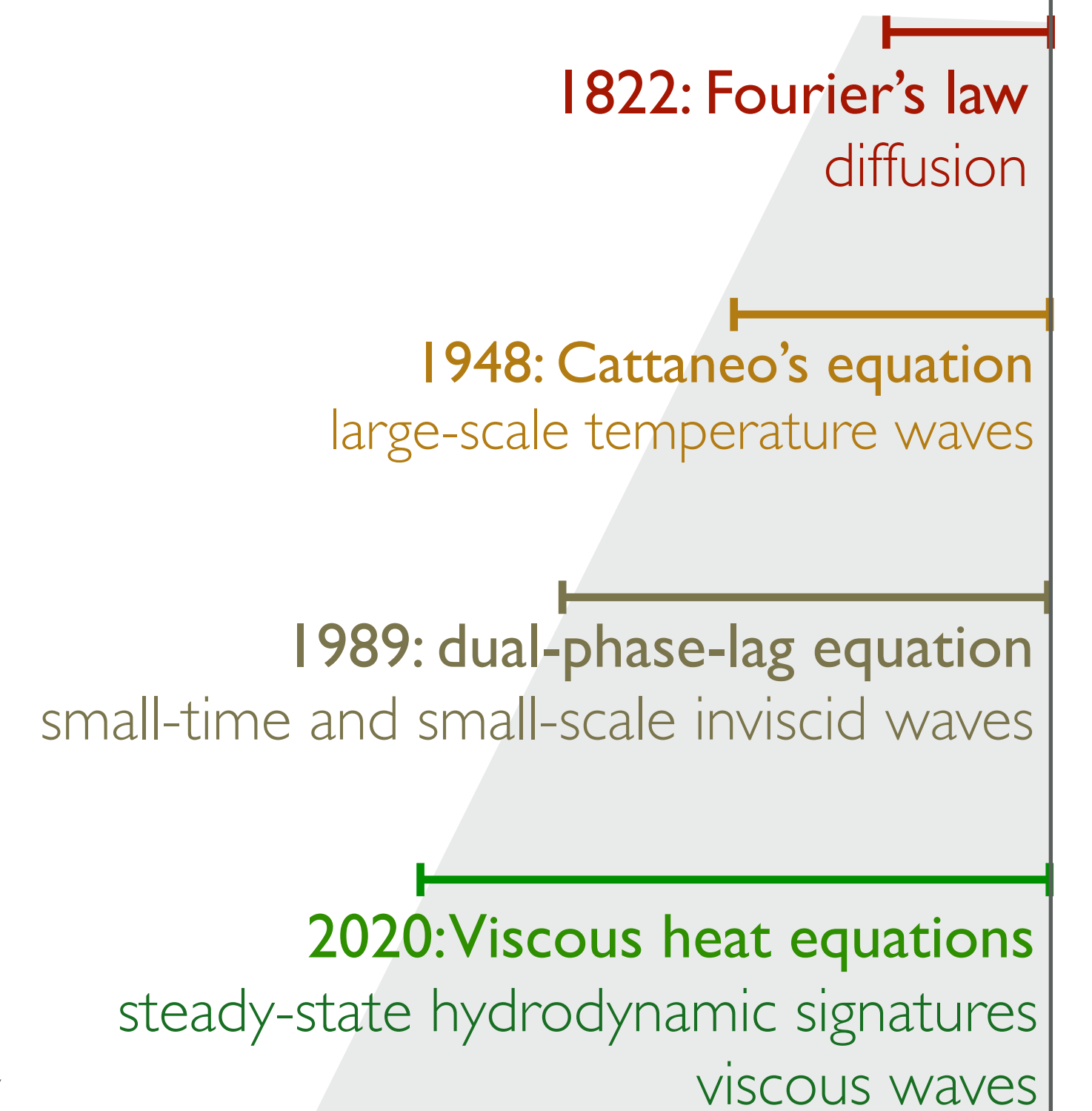
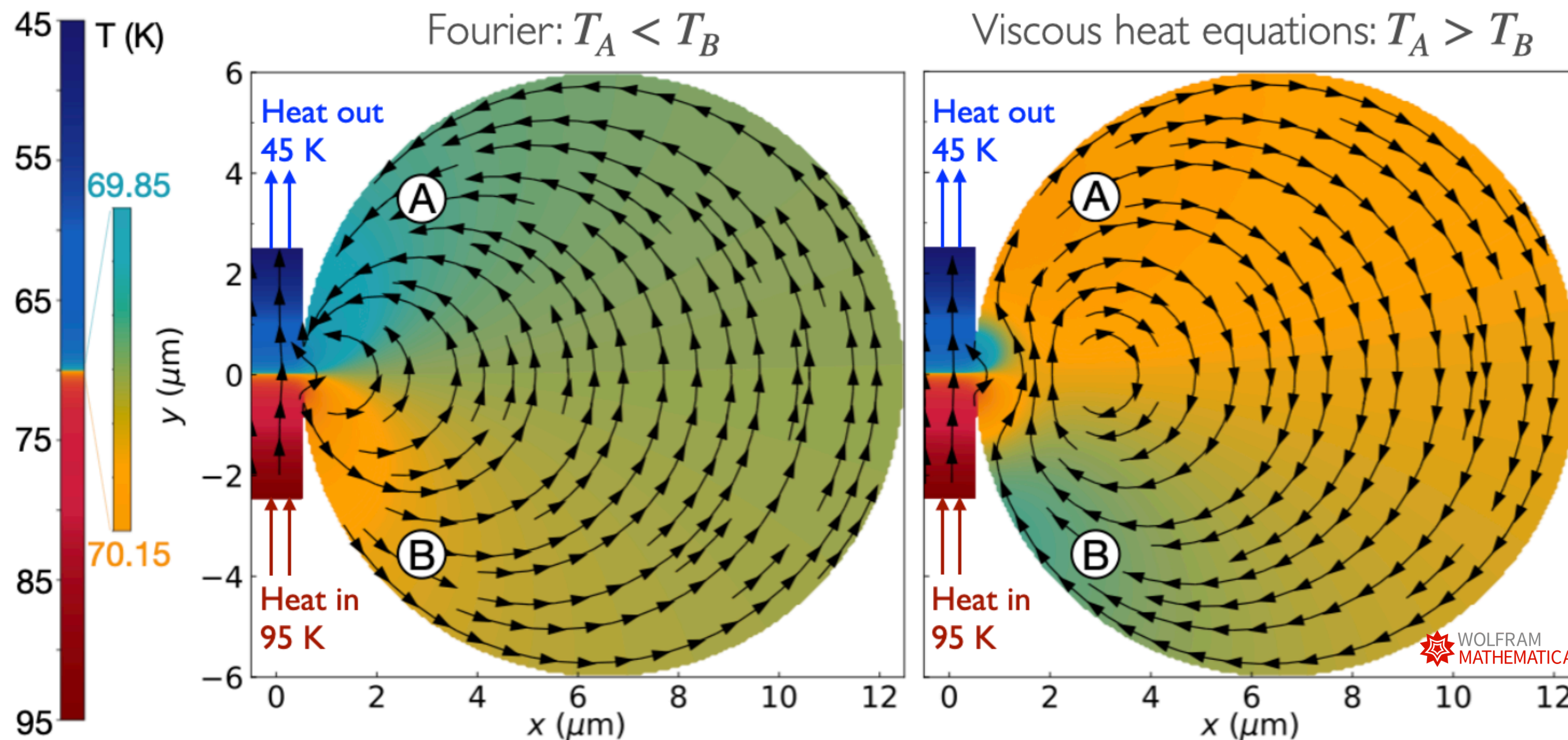
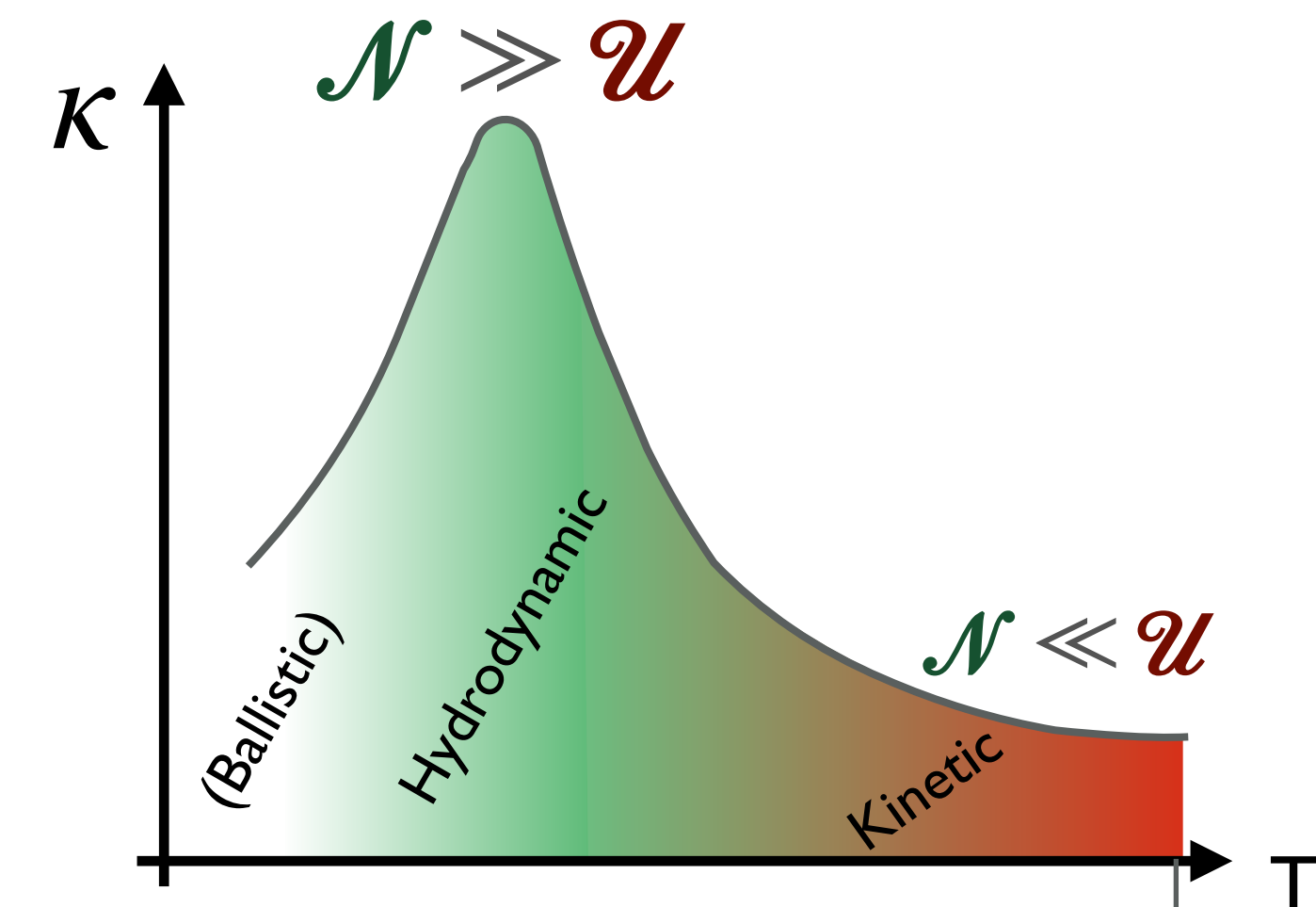
$$\kappa^{ij} = C \sum_{\alpha} w_{0\alpha}^i w_{0\alpha}^j \tau_\alpha$$

Cepellotti and Marzari, PRX 6 (2016)

VISCOUS HEAT EQUATIONS GENERALISE FOURIER'S LAW

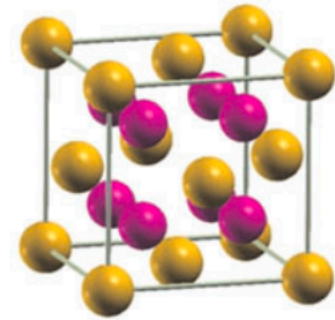
$$\partial_t T + \vec{A} \otimes \nabla_x \mathbf{u} - \vec{\kappa} \otimes \nabla_x^2 T = 0$$

$$\partial_t \mathbf{u} + \vec{B} \otimes \nabla_x T - \vec{\mu} \otimes \nabla_x^2 \mathbf{u} = -\vec{D} \otimes \mathbf{u}$$

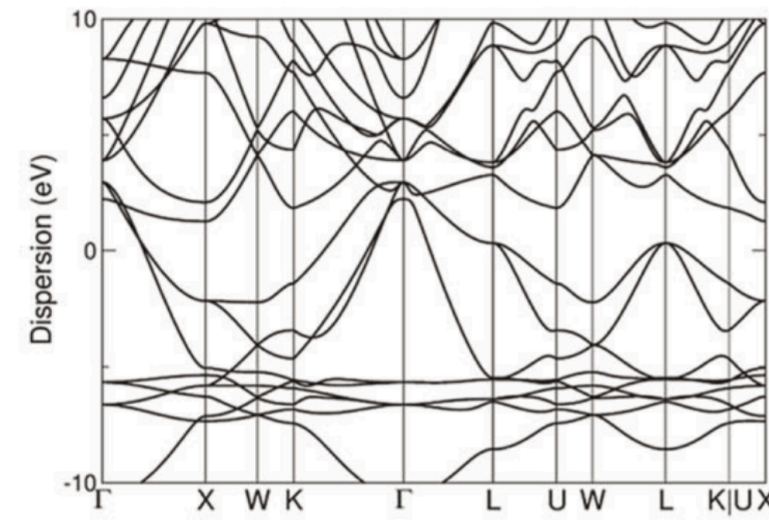


PREDICTING REFLECTIVITY AND COLOUR OF METALS

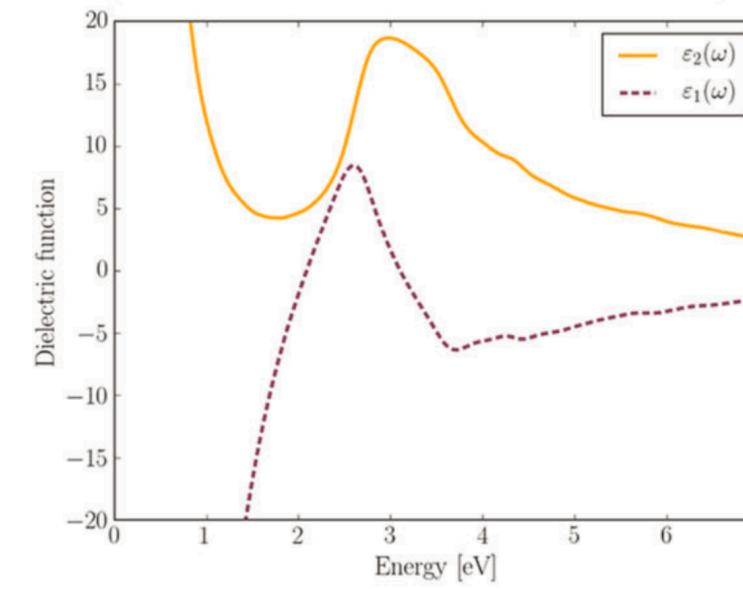
ColourWorkflow Crystal structure



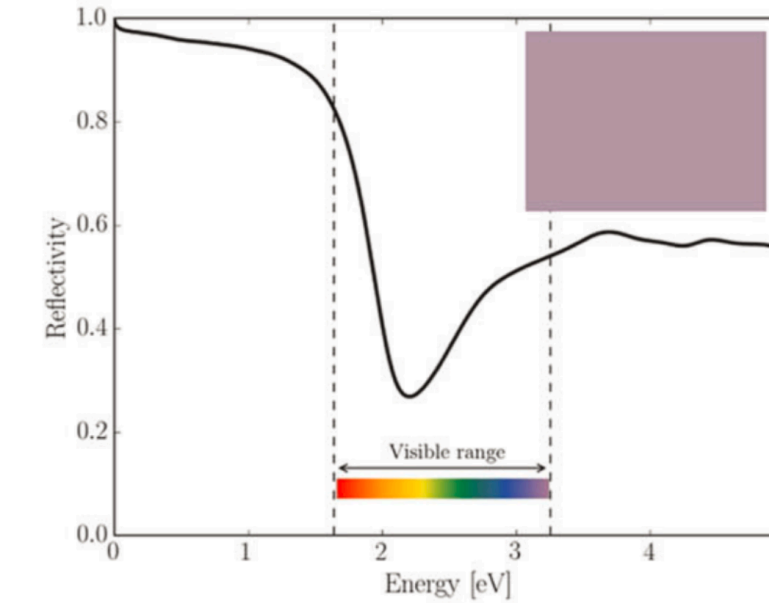
(i) Band structure



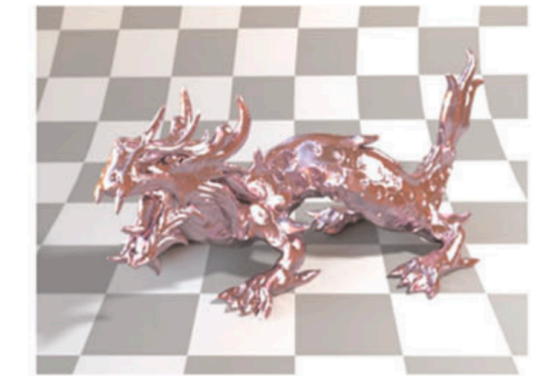
(ii) Dielectric function (interband + intraband)



(iii) Reflectivity and colour



(iv) Photorealistic rendering

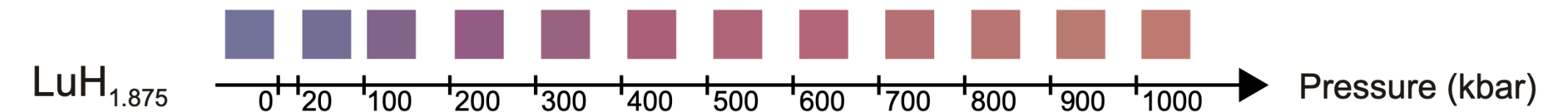


$$\epsilon(\hat{\mathbf{q}}, \omega) = 1 - \frac{4\pi}{V} \sum_{\mathbf{k}} \sum_{\substack{n,n'}} \frac{|\langle \psi_{n'\mathbf{k}} | \hat{\mathbf{q}} \cdot \mathbf{v} | \psi_{n\mathbf{k}} \rangle|^2}{(E_{n'\mathbf{k}} - E_{n\mathbf{k}})^2} \frac{f_{n\mathbf{k}} - f_{n'\mathbf{k}}}{\omega - (E_{n'\mathbf{k}} - E_{n\mathbf{k}}) + i\eta} - \frac{\omega_D^2(\hat{\mathbf{q}})}{\omega(\omega + i\gamma)}$$

$$\epsilon(\omega) = [n(\omega) + ik(\omega)]^2$$

$$R(\omega) = \frac{[n(\omega) - 1]^2 + k(\omega)^2}{[n(\omega) + 1]^2 + k(\omega)^2}$$

Prandini, Rignanese, & Marzari, *npj Comput. Mater.* 129 (2019)



Ab-initio theory predicts color change but no superconductivity

Kim, Conway, Pickard, Pascut, & Monserrat, *arXiv:2304.07326*

nature

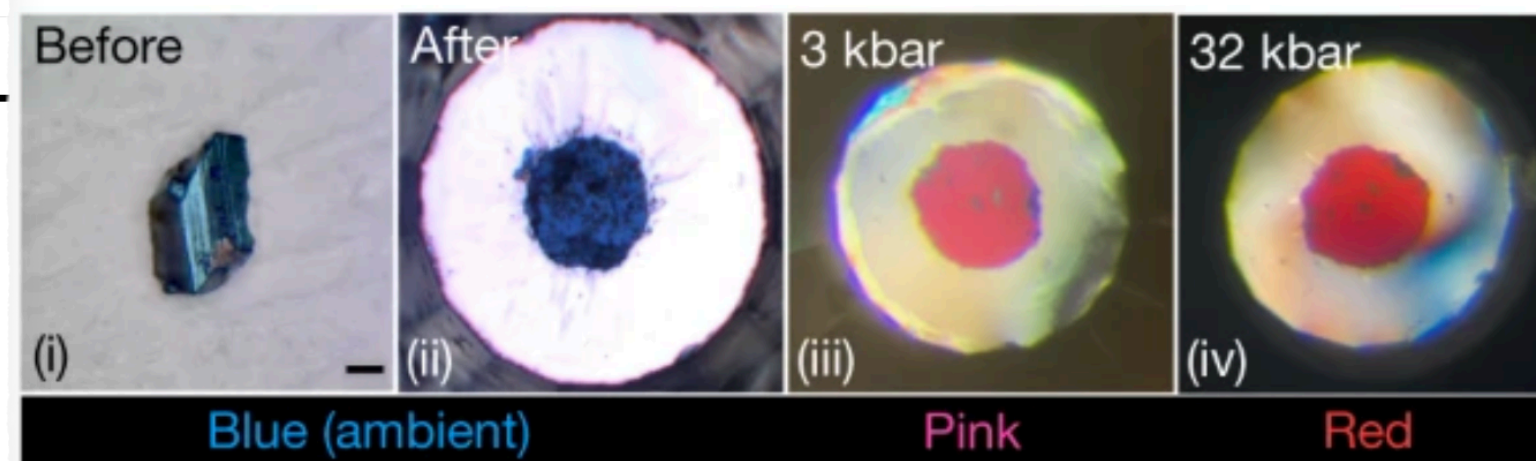
Explore content About the journal Publish with us

nature > articles > article

Article | Published: 08 March 2023

Evidence of near-ambient superconductivity in a N-doped lutetium hydride

Nathan Dasenbrock-Gammon, Elliot Snider, Raymond McBride, Hiranya Pasan, Dylan Durkee, Nugzari Khalvashi-Sutter, Sasanka Munasinghe, Sachith E. Dissanayake, Keith V. Lawler, Ashkan Salamat & Ranga P. Dias



nature

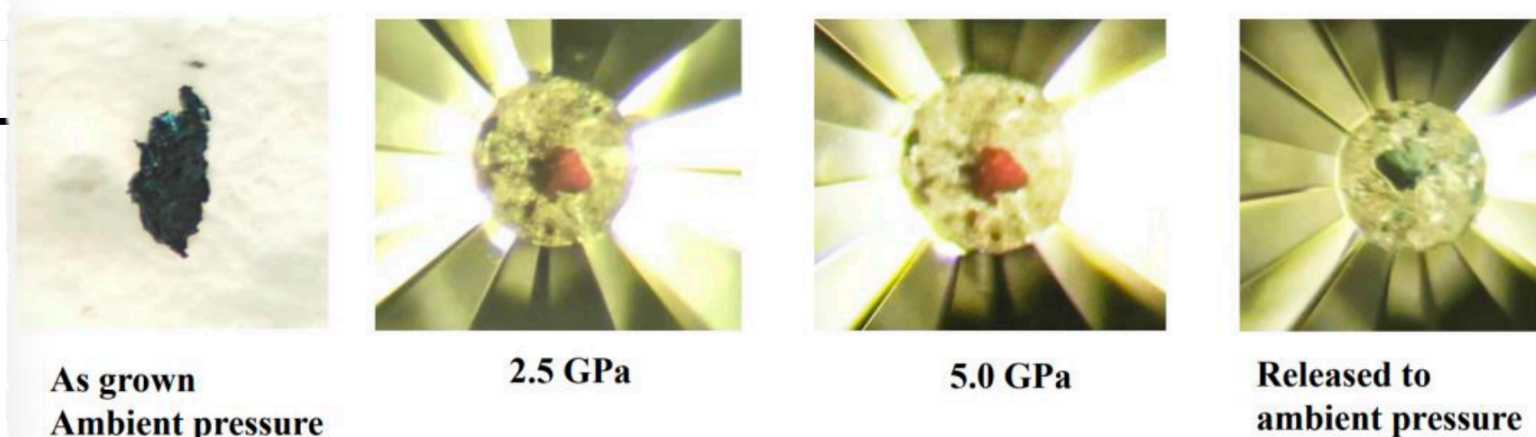
Explore content About the journal Publish with us

nature > articles > article

Article | Published: 11 May 2023

Absence of near-ambient superconductivity in LuH2-xNy

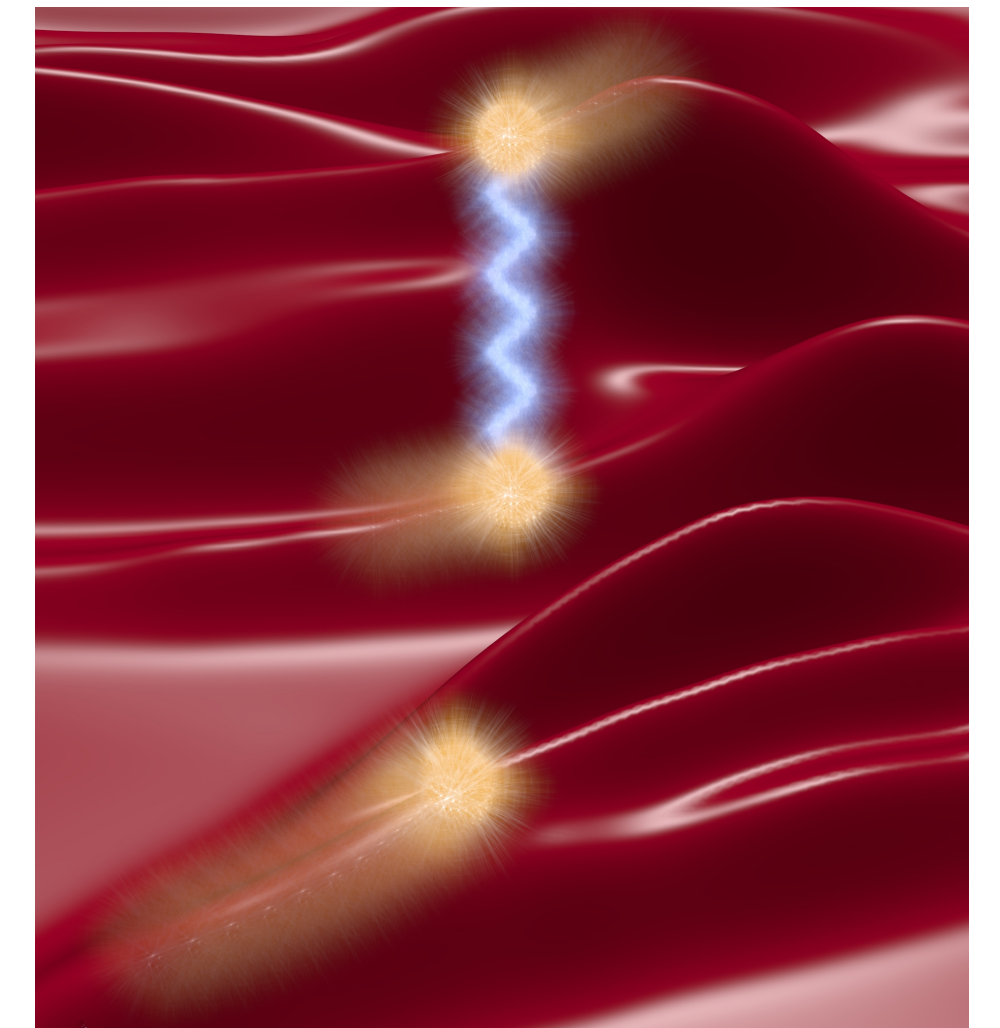
Xue Ming, Ying-Jie Zhang, Xiyu Zhu, Qing Li, Chengping He, Yuecong Liu, Tianheng Huang, Gan Liu, Bo Zheng, Huan Yang, Jian Sun, Xiaoxiang Xi & Hai-Hu Wen



CONCLUSIONS

 **QUANTUM ESPRESSO** allows to predict from first principles:

\AA — Bands for electrons and phonons, and **broadening** due to interactions;
nm — **electrical and thermal conductivity** beyond semiclassical theory;
 μm — Ionic diffusion or heat transport in **disordered materials**;
mm — **Raman spectra**, useful to characterise structural properties;
parameters for **mesoscopic models** for **devices**.



ms2855@cam.ac.uk

Acknowledgements

Prof. Marzari

Prof. Mauri

Dr Cepellotti

Dr Paulatto

Dr Harper

Dr Kahle

Dr Prandini

